Pryout Capacity of Cast-In Headed Stud Anchors

Neal S. Anderson, P.E., S.E.
Consultant
Wiss, Janney, Elstner Associates, Inc.
Northbrook, Illinois

Donald F. Meinheit, Ph.D., P.E., S.E.
Senior Consultant
Wiss, Janney, Elstner Associates, Inc.
Chicago, Illinois

Pryout is a failure mode for headed studs that occurs when short, stocky studs are used in an anchorage loaded in shear away from an edge. As part of a PCI research program, Wiss, Janney, Elstner Associates, Inc. (WJE) studied a number of testing programs reported in the literature. Pushoff tests of headed stud connections from the 1960s and early 1970s, focusing on composite beam design, were reviewed to determine the steel capacity of headed stud anchorages away from all edge effects. This extensive database was further evaluated to examine the pryout failure mode. As a result of a careful analysis of this historic data, a modified pryout formula rooted in a shear type failure mode is proposed. The database was also found to be lacking in pryout tests having a variable spacing parallel to the applied shear load. To further evaluate the effect, eight laboratory tests were conducted focusing on this variable. Six anchorages with four studs and two anchorages with six studs were tested to examine individual y-spacing and the overall Y-spacing projection of the anchorage. From these tests and others reported recently, the influence of y-spacing was evaluated, and a modification factor is proposed to the basic pryout capacity equation.

A review of the concrete anchorage design provisions in Appendix D of ACI 318-05[1] reveals that there are multiple failure modes for concrete anchorages in shear or tension. One such failure mode is the concrete pryout mechanism, which usually occurs for very shallowly embedded studs or post-installed anchors. Such short anchors are typically used in sandwich wall panels, where the anchor is cast in one thin wythe as shown in Fig. 1.[2] Current provisions of ACI 318 Appendix D[1] treat the pryout mechanism as a pseudo-tension pullout failure and use the tensile pullout capacity of Eq. D-4 modified by a factor k_{cp}. This treatment is discussed in detail further in this paper.

A review of the literature for headed studs indicates that the pryout failure mechanism is more of a subset of the shear failure mode, rather than tension. The shear mode is better represented by the AISC equation[3,4] for stud strength, derived from

the work of Ollgaard et al.[5] This equation was simplified by Shaikh and Yi[6] and later incorporated into the third and fourth editions of the PCI Design Handbook.[7,8]

This paper provides a review of the known pryout data on cast-in headed studs and anchor bolts. Tests focusing on this sole mechanism have been performed only by Hawkins[9] and Zhao.[10] In order to expand the database, the authors reviewed a number of pushoff test results used in the early development of composite beam design and tested in the 1960s and early 1970s.

These results greatly expand the test data available on pryout behavior. The authors' review provided additional insight into failure behavior by pryout that should not be ignored in light of anchorage design failure mechanisms.

PRYOUT MECHANISM

The pryout mechanism for cast-in anchors usually occurs with very short, stocky studs welded to a steel plate or beam flange. The studs are typically so short and stiff that under a direct shear load, they bend primarily in single curvature. The ensuing deformation results in the "heel" of the stud head "kicking back," which breaks out a crater of concrete behind the stud, as illustrated in Fig. 2.

Internal bearing pressures develop in the concrete near the concrete surface at the stud weld and at the stud head due to rotational restraint. This failure mechanism occurs away from all edge effects, when the anchorage is located "in-the-field" of the member. The behavior is somewhat analogous to a laterally loaded pile in earth.

A longer and less stiff stud behaves differently. The longer and deeper embedded stud bends in double curvature and the deeply embedded head portion of the stud remains essentially stationary or fixed in the concrete. At the junction of the headed stud and plate or flange, the projected stud diameter in front of the stud bears directly on the concrete near the surface and induces a zone of concrete crushing. If the connection is close to an edge, the concrete anchorage assembly will likely break out a concrete section due to the edge effects.

If the connection is located sufficiently away from the edge to preclude an edge breakout, the stud or studs will likely fail in a steel shear failure mode. As reported previously by Anderson and Meinheit[11,12] through a review of this data, the shear capacity of the stud group clear of the edge effects can be defined by:

$$V_s = n\, A_s f_{ut} \qquad (1)$$

where

V_s = nominal shear strength of a single headed stud or group of headed studs governed by steel strength (lb)
n = number of studs or anchors in a group
A_s = effective cross-sectional area of a stud anchor (sq in.)
f_{ut} = design minimum tensile strength of headed stud steel in tension (psi)

Currently, this equation is the same as Eq. D-17 of ACI 318-05 Appendix D,[1] without the capacity reduction factor, ϕ.

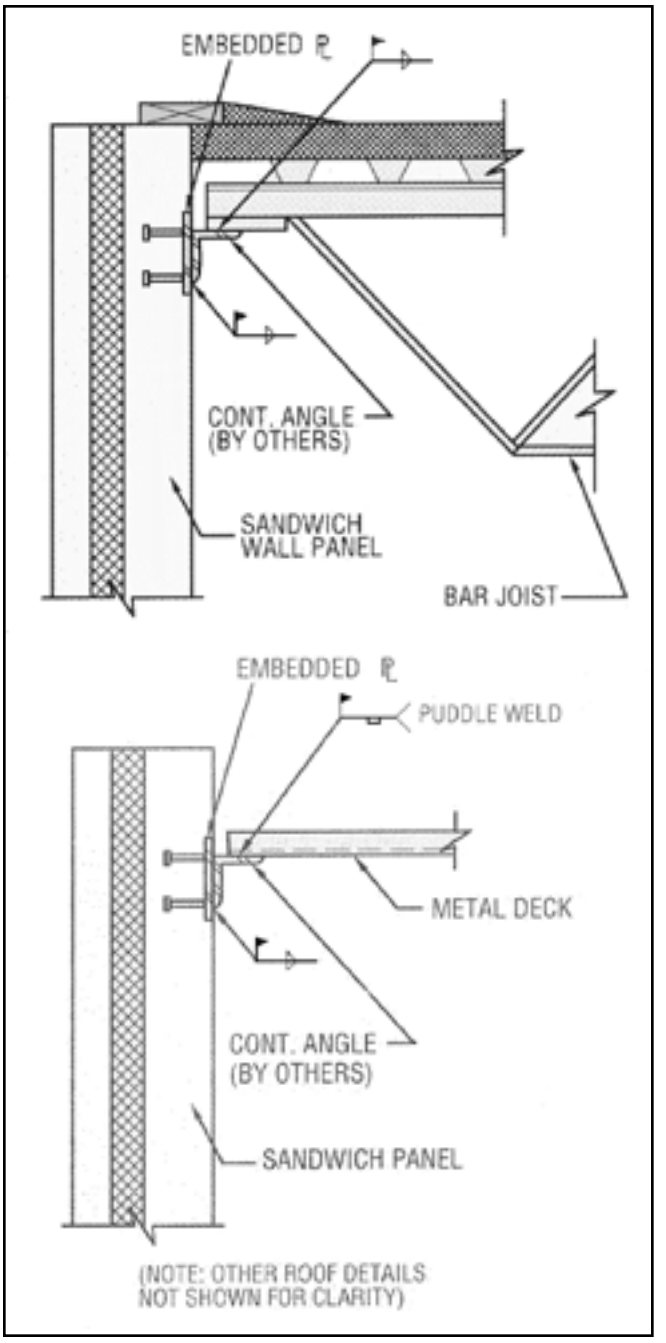

Fig. 1. Typical connections in precast sandwich wall panels influenced by short stud use.[2]

ACI 318-05 Appendix D Pryout Capacity

The ACI 318-05 Appendix D requirements for pryout capacity are based on the tensile concrete breakout model modified to account for shear. The ACI tensile concrete breakout method requires the effective embedment depth, h_{ef}, in the calculation of the breakout capacity. The breakout surface is computed using the effective area of the CCD physical breakout model.[13]

The provisions in ACI 318-05 Appendix D[1] are as follows:

The nominal pryout strength, V_{cp}, shall not exceed:

$$V_{cp} = n\, k_{cp} N_{cb} \qquad (2)$$

where

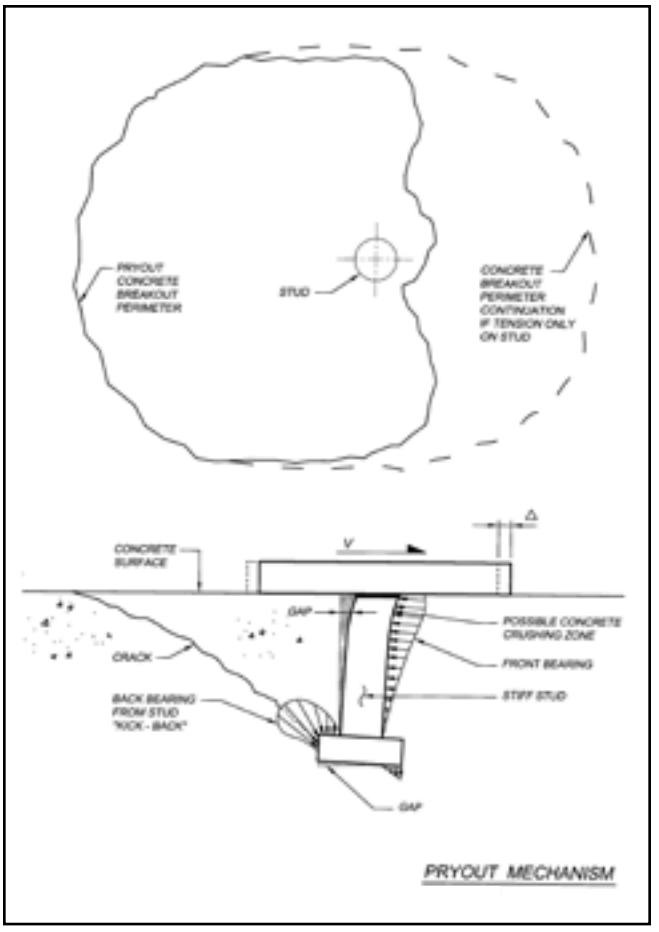

Fig. 2. Plan and cross section of the pryout behavior mechanism in a concrete member.

k_{cp} = coefficient for pryout strength
= 1.0 for $h_{ef} < 2.5$ in.
= 2.0 for $h_{ef} \geq 2.5$ in.
V_{cp} = nominal concrete pryout strength in shear (lb)
N_{cb} = nominal concrete breakout strength of a single anchor in tension (lb)

The notation N_{cb} is the concrete tensile breakout strength and is determined in accordance with the ACI 318 Appendix D requirements. The k_{cp} term is an empirical correlation coefficient that relates typical tension breakout to the pryout capacity. The correlation coefficient is a two-stage step function, depending on the embedment depth.

LITERATURE REVIEW

Pushoff Tests

Stud welding was developed in the 1930s at the New York Naval Shipyard for the purpose of attaching wood planking over the top metal deck surface of a ship. A threaded stud could be placed on the exterior side of the steel deck plate by one worker, rather than using two workers inserting bolts through drilled holes. The headed stud was developed shortly thereafter, and its application to the construction industry expanded.

The headed stud was viewed as an efficient and effective shear transfer device, replacing channels, angles, or fabricated spirals welded to the top flange of steel bridge beams in composite construction. Thus, the welded headed stud gained considerable research attention in the late 1950s and through the 1960s. The early research work on welded headed studs was focused on composite beam behavior (concrete slabs with steel beams), using both normal weight and lightweight

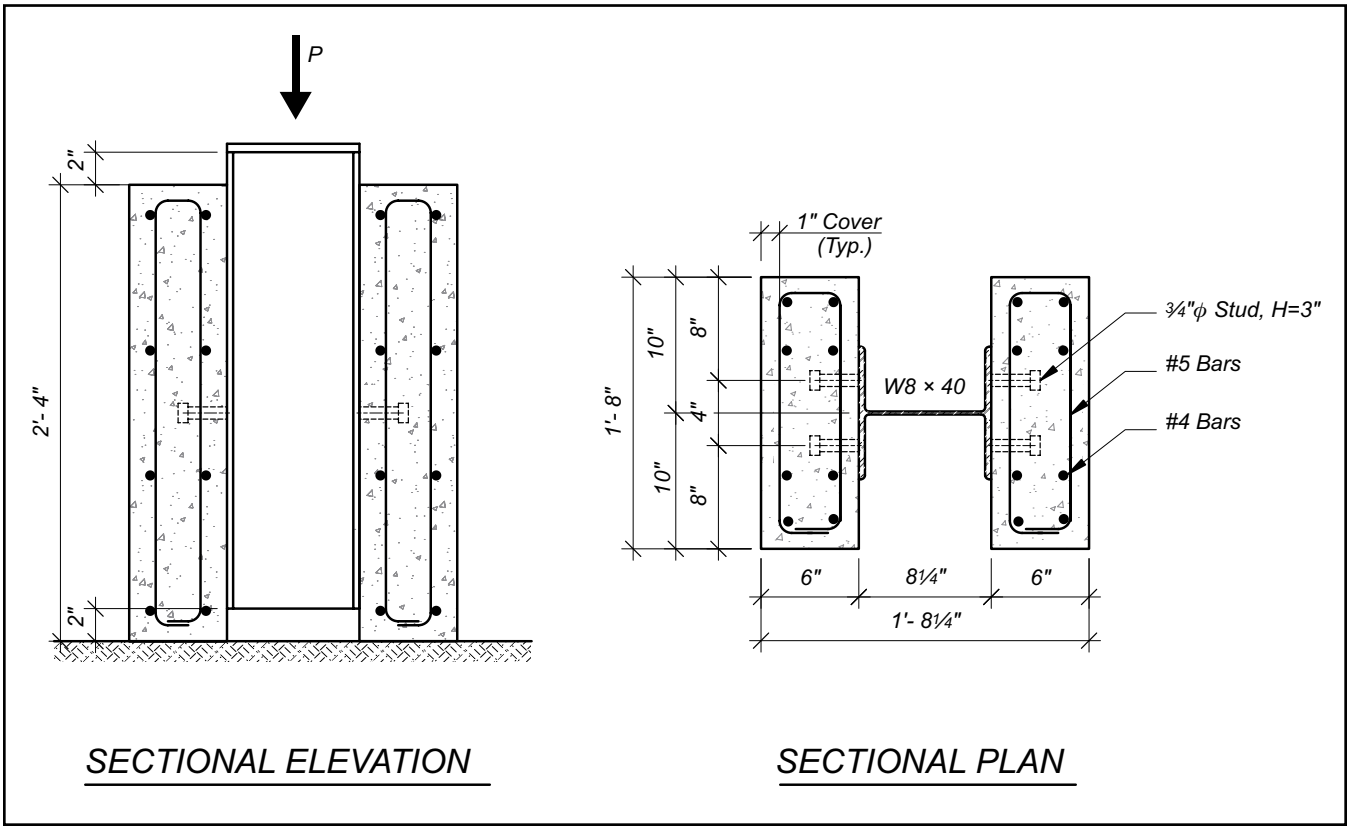

Fig. 3. Example of a pushoff specimen used by Ollgaard et al.[5]

concrete. Current research on headed stud applications range from metal decking to composite columns.

Early testing to evaluate composite beam behavior typically utilized a pushoff specimen to study shear transfer through the headed studs. The pushoff test specimen commonly used a wide flange beam section sandwiched between two slabs of concrete, modeling the deck slab of a composite beam. Headed studs at a prescribed spacing were welded to both flanges and typically embedded into a thin concrete slab representing the composite bridge deck slab.

The concrete slab was also usually reinforced to simulate typical conditions found in a bridge deck. As shown in Fig. 3, the steel beam was held above both the top and bottom elevation of the slabs. Both the beam and two slabs were oriented vertically, thus conveniently fitting into a Universal Testing Machine.

Early composite beam research, using the pushoff specimen, was conducted by Viest[14] at the University of Illinois; Driscoll and Slutter[15] and Ollgaard et al.[5] at Lehigh University, Baldwin et al,[16] Baldwin,[17] Buttry,[18] Dallam,[19,20] and others at the University of Missouri-Columbia; Goble[21] at Case Western Reserve University; Dhir[22] and Steele[23] under the direction of Chinn[24] at the University of Colorado; Davies[25] at the University of London; and Hawkins[26] at the University of Sydney. These early test programs produced a significant amount of shear data, mostly on group effect behavior of headed studs.

A review of the pushoff test results was conducted as part of the PCI research project reported by Anderson and Meinheit[11] because it provides good comparative data for headed studs loaded in pure shear. Prior to that PCI project, previous testing on headed stud connections as used in precast concrete type attachments was limited, especially when groups were considered.

As noted in the paper by Anderson and Meinheit,[11] the pushoff test specimen design has characteristics limiting its capability to emulate a precast concrete anchorage. The thin concrete slabs used in pushoff tests generally contained reinforcement representative of bridge deck construction. The reinforcement amount had no influence on the load to cause first cracking, but the reinforcement in the concrete slab likely held the slab together to allow for additional slip displacement and ductility.

Early researchers also were particularly concerned with load-slip characteristics of the headed stud connection. Unreinforced concrete specimens, reported in the literature, oftentimes produced a splitting failure in the concrete slab, a failure mode unlikely to occur in actual bridge deck construction because of the presence of transverse reinforcement. Work by Oehlers[27] and Oehlers and Park,[28] with a slightly modified single-sided, pushoff type specimen, focused on a longitudinal splitting mechanism—that is, splitting parallel to the shear force.

Another pushoff specimen limitation exists in the way the specimen applies load to the embedded studs. Load being transferred from the steel beam through the headed studs into the two concrete slabs results in the best theoretical condition to place the studs in pure shear. However, the externally applied load causes a compression on the concrete slab ends where they bear on the platen of the test machine.

This confinement condition is viewed to be analogous to a headed stud anchorage located *in-the-field* of a member; that is, a significant amount of concrete slab is located in front of the anchorage to preclude any front edge breakout influence.

The favorable concrete compression stress developed in front of the studs does not affect tests having one transverse row (or one *y*-row) of studs. However, when stud groups with multiple longitudinal rows were tested using the pushoff specimen, the test results became more difficult to interpret. Each longitudinal row in the group is subjected to a different level of compressive confinement stress.

Likewise, multiple longitudinal (or *y*-) rows spaced at large distances reduce the efficiency of the anchor group due to shear lag effects, similar to a long bolted connection.[29] Experimental testing reported herein by the authors was performed to study multiple *y*-rows and the shear lag influence.

Pryout Tests

Most laboratory testing programs intent on studying anchorages in shear have been conducted by loading the connection in shear toward a free edge and failing in a concrete breakout mode. Published test results on headed stud groups loaded in pure shear without the influence of any edge effects is limited to the work reported by Hawkins[9] and Zhao.[10]

University of Washington—In the early 1980s, research on embedded anchor bolts loaded in shear was conducted at the University of Washington, as reported by Hawkins.[9] This work studied the shear and tensile strength of single cast-in-place anchor bolts embedded in concrete slabs. The testing

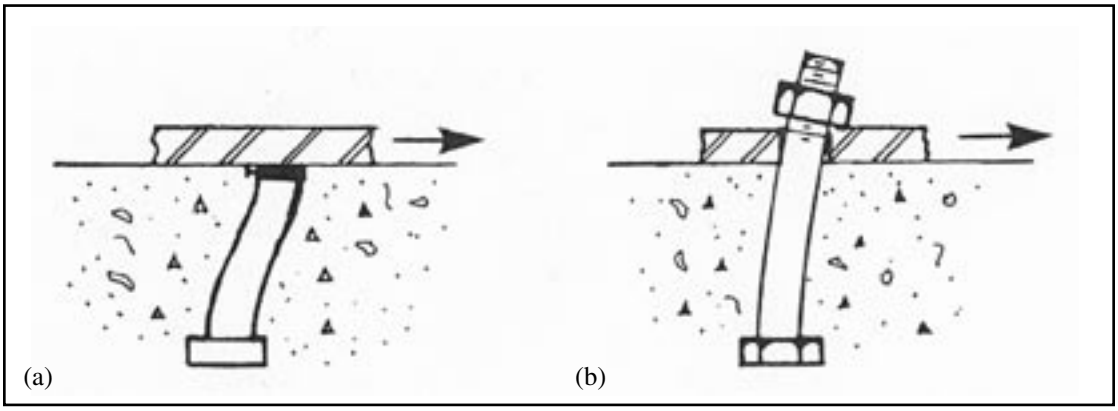

Fig. 4. End fixity conditions at the connection plate:[9] (a) Headed stud weld produces a fixed condition; (b) Post-installed anchor in a hole allows rotation, making a pinned condition.

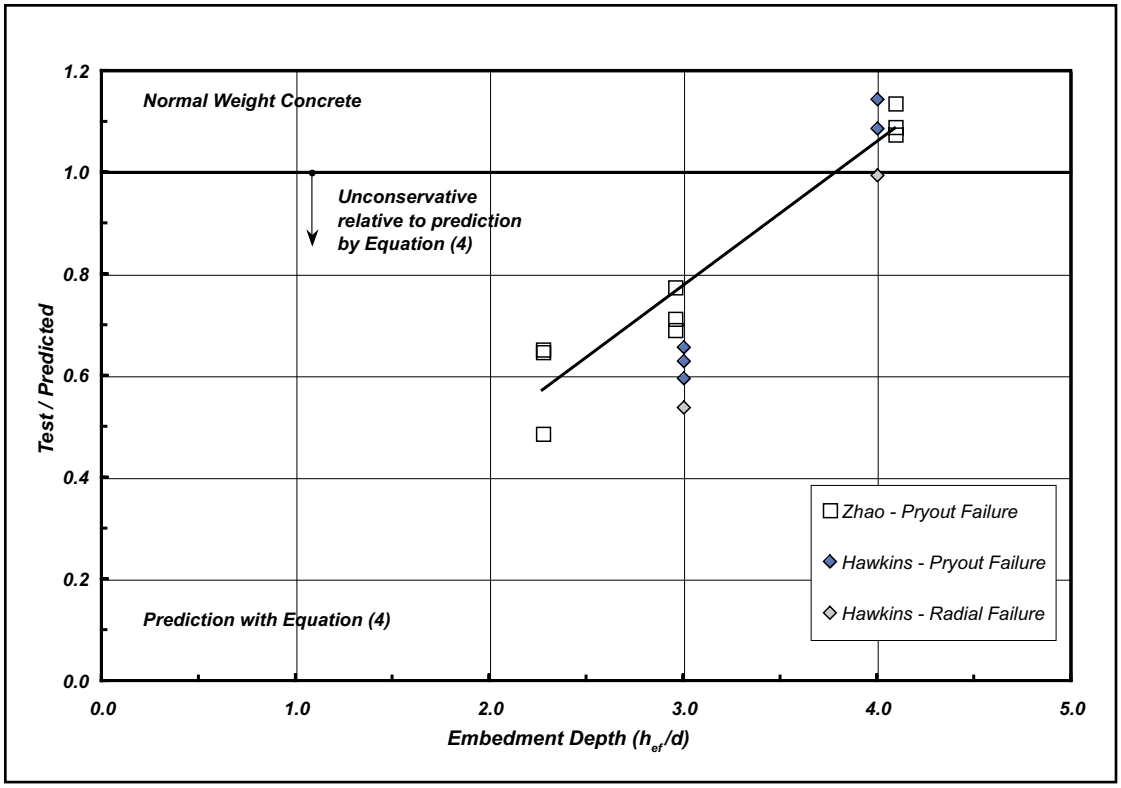

Fig. 5. Test-to-predicted capacity versus embedment depth using Eq. (4) for the Hawkins[9] and Zhao[10] pryout test data.

program was intended to examine capacity design formulas to determine the best predictor of anchor bolt capacity. Comparisons were made with the PCI Design Handbook, Second Edition,[30] the AISC Steel Manual, Eighth Edition,[31] and Uniform Building Code (UBC)[32] design procedures.

Fifteen direct shear tests were conducted as part of the Hawkins work. Anchor bolts had mechanical properties of conventional A325 bolts.[33] Tested bolt diameters were ¾ or 1 in. (19 or 25 mm), and the concrete strength ranged from 3000 to 5000 psi (20.7 to 34.5 MPa). The bolt embedment depths were 3, 5, or 7 in. (76, 127, or 178 mm) to the top of an embedded washer. Each bolt was provided with a ⅝ in. (15.9 mm) thick washer at the formed head of the bolt, which had a diameter of 2, 4, or 6 in. (51, 102, or 153 mm). Tests were conducted on these single anchor bolts embedded in 1 ft 6 in. (457 mm) square concrete panels, each 9 in. (229 mm) thick.

Hawkins identified two failure modes in this shear testing: shear-cone pullout and radial cracking failures. The shear-cone pullout failure (pryout failure) was only observed for bolts with a 3 in. (76 mm) embedment depth, or an h_{ef}/d ratio of 4 or less. The radial cracking mode occurred with the longer embedments, and cracking appeared to be a function of the specimen size and test setup.

In his data analysis, Hawkins identified the load-slip characteristics of headed studs and anchor bolts as being different, as depicted in Fig. 4. An anchor bolt connection had comparatively more slip than a similar diameter headed-stud connection; this condition was attributed to the difference in the fixity of the anchor to the top plate. Because the stud attachment occurs through a weld, it provides a more rigid, or fixed, connection to the plate through which the anchor shear force is applied. Rotation is restricted with the headed-stud connection.

Alternately, an anchor bolt provides a semi-pinned, or semi-fixed, connection that has a degree of "softness;" thus, there is a capability of an anchor bolt to rotate at the plate on the surface more than a headed stud welded to the plate.

For the ¾ and 1 in. (19 and 25 mm) diameter anchor-bolt connectors used in the Hawkins study, it was concluded that the headed stud strengths were more than the anchor-bolt strengths for a similar embedment-to-diameter ratio (h_{ef}/d). At an h_{ef}/d ratio of about 4, a change in failure mode for the anchor bolts was observed. This ratio is similar to the h_{ef}/d ratio for headed studs needed to change the mode of failure of the anchorage loaded in shear.

University of Stuttgart (Germany)—As part of an extensive headed-stud testing program, Zhao[10] tested a number of single- and four-stud connections in pryout. The primary variable in the test series was the stud embedment depth. Three stud lengths were used, all yielding h_{ef}/d ratios less than 4.5. The three effective stud lengths, h_{ef}, were 1.97, 2.56, and 3.54 in. (50, 65, and 90 mm), and concrete pryout failures occurred with all of these stud lengths. For all tests, the stud diameter was held constant at a nominal ⅞ in. (22 mm).

A fourth effective stud length was used in two single-stud tests. The stud length was 4.53 in. (115 mm) and steel failure occurred in both tests. The h_{ef}/d ratio for these studs was 5.23. In the four-stud tests, the x- and y-spacing of the studs was a constant 3.94 in. (100 mm), making a square anchorage pattern. Only the stud lengths varied in the four-stud tests.

From the data analysis, Zhao[10] postulated the concrete breakout failure surface to be similar to a truncated tension breakout shape. Consequently, the prediction equation was based on a tensile pullout equation. The effective breakout area, A_n, from the ACI 318 Appendix D model was not centered or concentric about the anchorage; rather, the break-

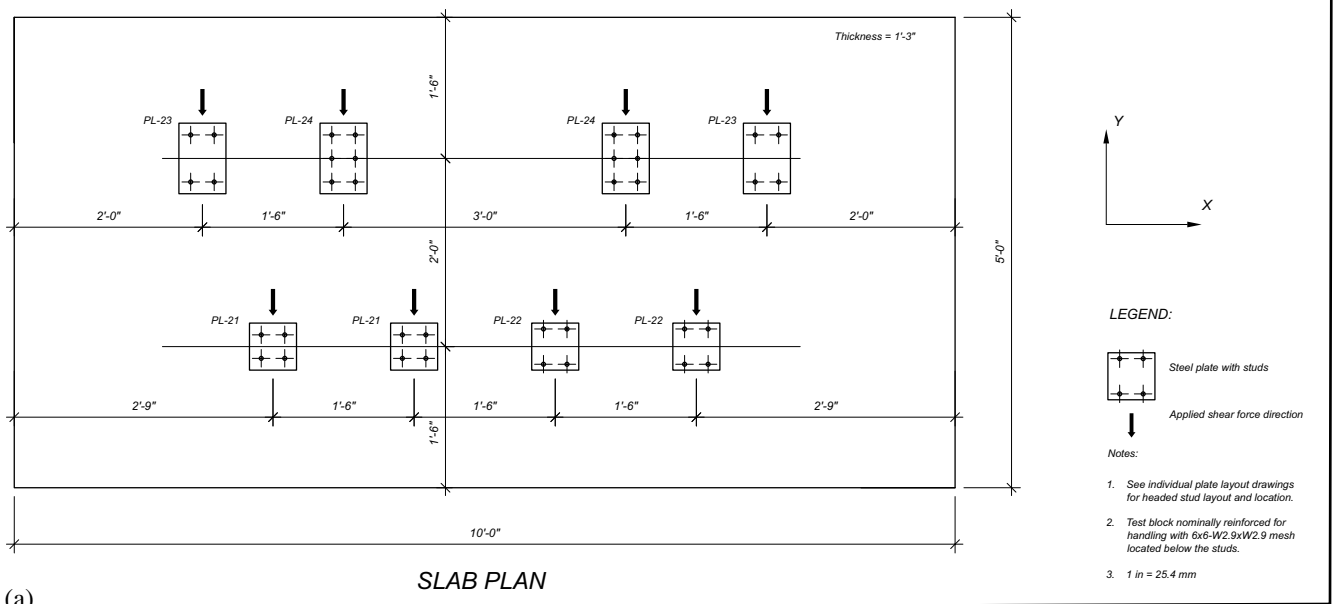

SLAB PLAN

(a)

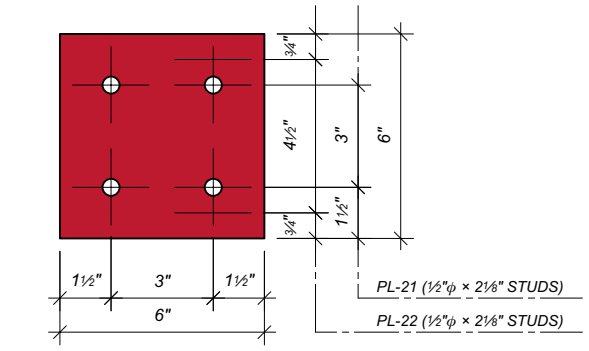

PL-21 & 22

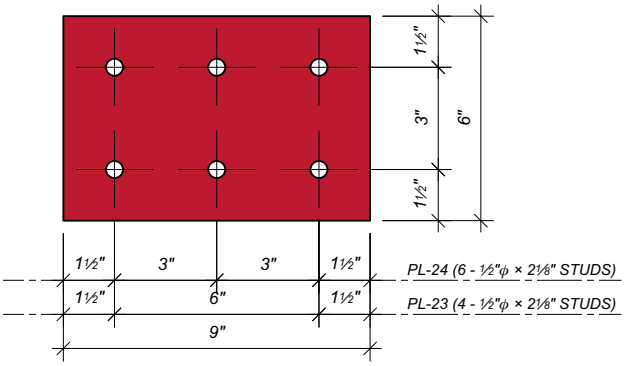

PL-23 & 24

(b)

Fig. 6. Layout of the WJE test slab and plate details used for the testing: (a) Slab plan; (b) Anchorage plate details.

out was shifted to a position behind the anchorage. Zhao proposed failure surface dimensions at the concrete surface based on the surface breakout angle, α, but only behind the anchorage.

The Zhao study later was formulated into the ACI 318 Appendix D provisions. In the Appendix D equations, the effective area, A_n, in the tensile pullout equation is assumed to be centered about the anchorage with a 35-degree breakout angle. As discussed previously in this paper, this design equation is modified by a constant (1 or 2) based on the stud embedment depth.

LITERATURE ANALYSIS

Keeping the limitations of the pushoff test in perspective, some valuable data are applicable to the present study on pryout. Relevant findings from these early tests regarding the basic influential anchorage parameters are discussed below.

Embedment Depth

In a previous paper, Anderson and Meinheit[11] studied the influence of the embedment depth ratio, h_{ef}/d, and its effect on breakout strength. Viest[14] ran a series of tests with variable stud diameters and reasonably constant effective embedment depths. This early data helped identify the occurrence of the pryout failure mode. After studying a number of pushoff tests and the failure modes, the authors concluded that cast-in headed studs with h_{ef}/d greater than or equal to about 4.5 failed in a steel stud shearing mode in normal weight concrete; the shear capacity would be calculated with Eq. (1). This h_{ef}/d value is slightly greater than the value of 4.2 identified by Driscoll and Slutter[15] and incorporated into the 1961 AASHO Specifications.[34]

Stocky studs, those defined with h_{ef}/d less than 4.5, oftentimes failed in a concrete pryout failure mode in normal weight concrete. In lightweight concrete, the delimiting ratio for h_{ef}/d ranges from 5.4 to 7.4, depending on the lightweight aggregate type, unit weight, and tensile strength of the concrete.

x-Spacing Effect

Section D.8.1 of ACI 318-05[1] provides for a minimum center-to-center anchor spacing of 4*d*. This influence has not been studied extensively in the literature. The work by Viest[14] confirms that steel stud failure can occur with an *x*-spacing (s_1) of 4*d* or greater. Closer spacings were shown to decrease capacity and hence the ACI minimum is a reasonable spacing requirement. Moreover, closer spacings with headed studs become impractical because of stud-gun clearances and stud head interferences.

Minimum Slab Thickness

Concrete pryout and steel stud failures loaded in shear in the pushoff specimens were achieved in relatively thin slabs. Pushoff data indicate that steel failures occurred in slabs ranging in thickness from 4 to 7 in. (102 to 178 mm). For the referenced tests herein, the clear cover over the stud head on the free surface side of the slab ranged from 1.0 to 3.1 in. (25 to 79 mm).

No definitive conclusions can be garnered from the existing pushoff data regarding minimum slab thickness. Because the bottom plane of the breakout surface for pryout forms at the stud head level, it is concluded that slab thickness is not a variable that influences the pryout failure load, assuming that nominal concrete cover is maintained over the stud heads. This result is also consistent with the ACI tension breakout model, whereby thickness is not an influence on the tension breakout capacity.

Past Prediction Equations

Ollgaard et al.[5] at Lehigh University conducted an extensive study using short studs with an effective embedment depth, h_{ef}/d, of 3.26 and different types of lightweight and normal weight concrete. Both stud steel shear and a concrete mechanism failure were reported; in some cases, both modes occurred simultaneously. Results from this testing produced a prediction equation, independent of failure mode, basing individual stud strength on stud area, concrete compressive strength, and elastic modulus of the concrete.

Their final simplified prediction equation for the average strength was:

$$Q_u = 0.5A_s\sqrt{f'_c E_c} \tag{3}$$

where

Q_u = nominal strength of a shear stud connector embedded in a solid concrete slab (kips)
A_s = effective cross-sectional area of a stud anchor (sq in.)
f'_c = specified compressive strength of concrete (ksi)
E_c = modulus of elasticity of concrete (ksi)

With the elastic modulus, E_c, Eq. (3) is applicable to both normal weight and lightweight concrete. Unlike earlier prediction equations from the pushoff test, this equation did not set applicability limits on the h_{ef}/d ratio.

Eq. (3) set the standard for pryout prediction. Post-1971 research studies referred to, and were calibrated to, this equation. The simplicity and good prediction characteristics of this equation have seen its widespread use in the AISC Specifications[3,4] since the late 1970s. In the AISC Specifications, the upper bound on the stud strength is $A_{sc}F_u$, where A_{sc} is the cross-sectional area of a stud shear connector and F_u is the minimum specified tensile strength of the stud shear connector.

In the mid-1980s, a simplified lower bound form of the Ollgaard et al. equation[5] was proposed by Shaikh and Yi[6] and adopted by PCI. This equation took the following form:

$$V_{nc} = 800\lambda A_s\sqrt{f'_c} \tag{4}$$

where

V_{nc} = nominal shear strength (lb)
A_s = effective cross-sectional area of a stud anchor (sq in.)
f'_c = specified compressive strength of concrete (psi)
λ = concrete unit weight factor

The Shaikh and Yi equation[6] used λ for grouping different classes of lightweight aggregate concrete based on sand replacement. The conversion of Eq. (3) to Eq. (4), with its assumptions and use of λ for lightweight aggregate concrete, resulted in a revised average prediction equation. Consequently, Shaikh and Yi selected a lower

Table 1. Material properties for concrete.

(1)	(2)	(3)	(4)	(5)	(6)
Concrete age (days)	**Average values (6 × 12 in. cylinders)**				**Notes**
	f'_c (psi)	**Static modulus E (× 10^6 psi)**	**Tensile strength f_{sp} (psi)**	**η**	
14	5390	—	—	—	
23	5840	4.06	485	6.3	Start testing
28	5920	4.22	—	—	
45	6300	4.17	581	7.3	Finish testing
Average		4.15			

Notes:
Concrete compressive strength, f'_c, is based on the average of three 6 × 12 in. test cylinders.
For Column (5), $f_t = \eta(f'_c)^{0.5}$
Concrete unit weight, γ = 150.9 lb per cu ft.
1 in. = 25.4 mm; 1000 psi = 6.895 MPa; 1 lb per cu ft = 16.026 kg/m³.

bound line of the data, resulting in the constant of 800. Eq. (4) appeared in both the third and fourth editions of the PCI Design Handbook[7,8] as a cap on anchorage capacity, independent of embedment depth.

DERIVATION OF A REVISED SINGLE *y*-ROW EQUATION

Both the Ollgaard et al.[5] and Shaikh and Yi[6] equation proposals incorporated the concrete compressive strength and a stud stiffness term through the use of the cross-sectional area, A_b. Through geometry, A_b indirectly incorporates the stud diameter modified by the constants 0.25 and π. The database that these equations were based on had embedment depth ratios, h_{ef}/d, of 3.25 to 4.67 for normal weight concrete tests. This range of embedment depth ratios represented the lower end of stud sizes most likely used in composite construction at the time (the 1980s). However, the two equations did not account for the stud embedment depth in this relatively narrow data range.

The influence of stud embedment depth is illustrated in Fig. 5 for the tests by Hawkins[9] and later by Zhao.[10] This plot shows test-to-predicted capacity versus h_{ef}/d, where the predicted capacity is based on Eq. (4). Both researchers used cast-in anchors with h_{ef}/d ratios at the low end of the available headed studs in the manufacturer's catalog, providing data for h_{ef}/d ratios of 2 to 4.

The trend of the data shown in Fig. 5 illustrates that an increasing embedment depth ratio increases the pryout capacity. With respect to the Eq. (4) predictor, a lower h_{ef}/d ratio reduces the prediction capacity, such that Eq. (4) is unconservative (< 1.0).

When the Hawkins and Zhao pryout data are added to the database of pushoff tests, the trend and influence of embedment depth is better defined and the data from the pushoff tests follow the same trend. Using linear multi-variable regression analysis to analyze the data, the following equation is derived for a single stud or a single *y*-row line of studs:

$$V_{poc} = 317.9\lambda\, n \sqrt{f'_c}\,(d)^{1.5}(h_{ef})^{0.5} \le nA_{se}f_{ut} \qquad (5)$$

The concrete breakout equation for pryout is:

$$V_{po} = \phi V_{poc}\psi_y \le nA_{se}f_{ut} \qquad (6)$$

and the 5 percent fractile value is thus defined:

$$V_{poc} = 215\lambda\, n \sqrt{f'_c}\,(d)^{1.5}(h_{ef})^{0.5} \qquad (7)$$

where

V_{po} = nominal pryout shear strength (lb)
V_{poc} = nominal pryout shear strength for one *y*-row of anchors (lb)
A_{se} = effective cross-sectional area of stud anchor (sq in.)
d = nominal anchor diameter (in.)
h_{ef} = effective embedment depth of cast-in anchor (in.)
f'_c = specified compressive strength of concrete (psi)
f_{ut} = design minimum tensile strength of headed stud steel in tension (psi)
n = total number of anchors in connection
λ = concrete unit weight factor per ACI 318
ψ_y = *y*-spacing factor (defined later in this paper)

Eq. (5) was derived using 65 tests from both pushoff and pryout testing programs. With this database, the mean is 1.00, the standard deviation is 0.166, and the coefficient of variation (COV) is 16.5 percent. In accordance with Wollmershauser,[35] the 5 percent fractile reduction is presented as Eq. (7) for uncracked concrete.

Similar to past versions of a pryout equation in PCI form, Eq. (7) includes the unit weight factor λ for lightweight aggregate concrete. Eq. (7) was also evaluated with a database

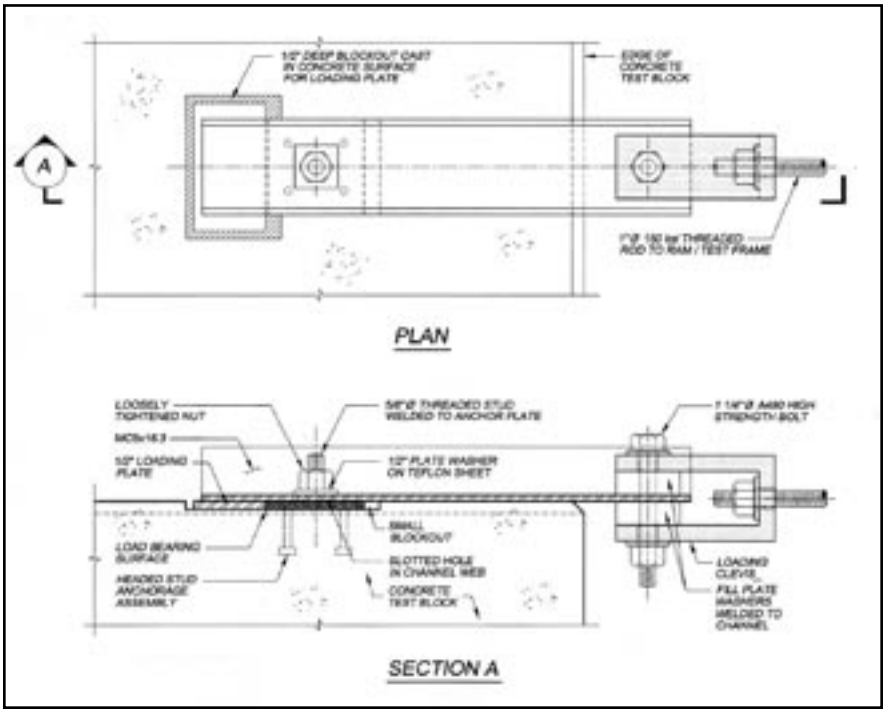

Fig. 7. Detail of the WJE test load application apparatus.

Fig. 8. Overall view of the WJE test setup in the laboratory.

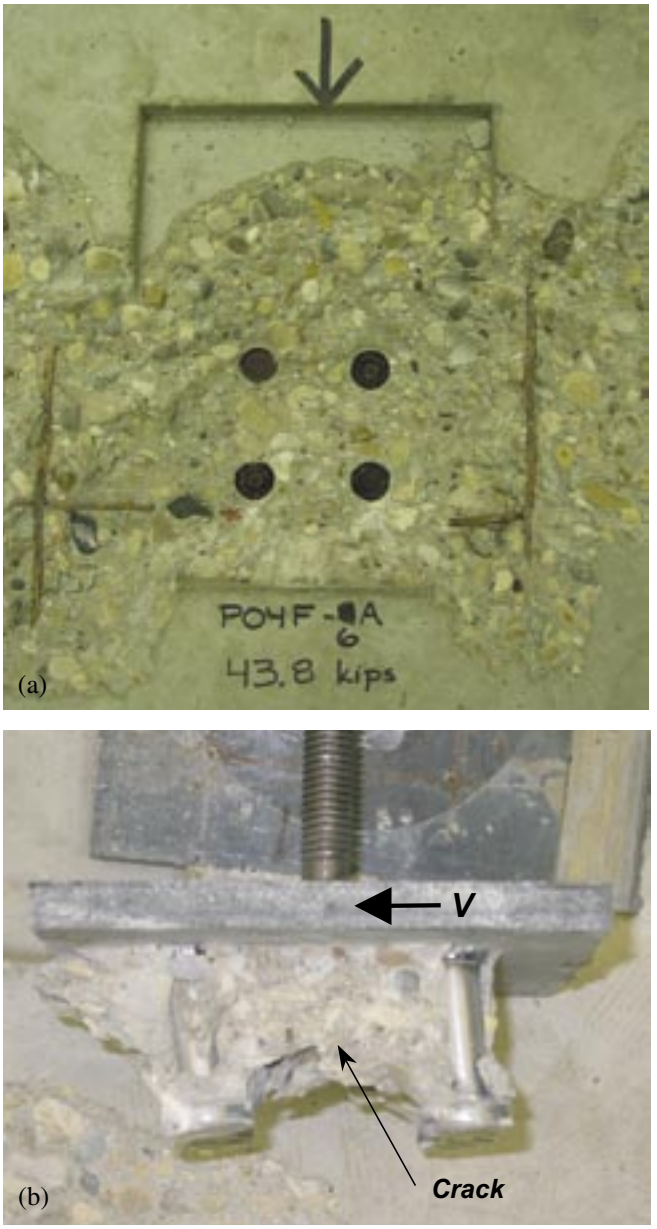

Fig. 9. Failure conditions of Test PO4F-6A with $y = 3$ in. (76 mm): (a) Concrete breakout plan on slab; (b) Connection plate with concrete intact.

of 78 lightweight aggregate concrete tests failing in a concrete mode and found to be a reasonably good predictor using λ instead of the elastic modulus. The statistics for the lightweight aggregate concrete database of 78 tests revealed a mean of 1.07, a standard deviation of 0.195, and a COV of 18.3 percent. The statistics show an increased scatter of lightweight aggregate concrete test results, yet the COV is comparable to that of the normal weight concrete data set.

Appendix B presents the entire database table for the 225 tests used for analysis, including the 65 normal weight and 78 lightweight concrete tests. The database tables in Appendix B warrant explanatory notes with respect to lightweight aggregate concrete and the noted failure mode definition.

The lightweight concrete tests listed in Appendix B reported various concrete properties in order to classify its lightweight category. These tests often preceded the advent of the ACI λ factors for lightweight concrete and, therefore, λ was not used. For the database presented herein, an interpolated λ factor was used, if possible, derived from the split cylinder data.

If little information was provided on the lightweight concrete properties, an ACI value of 0.75 or 0.85 was used based on reported concrete density or information in the paper text. This is consistent with Sections 11.2.1.1 and 11.2.1.2 of ACI 318-05. The λ factor thus determined was used to appropriately modify Eq. (7) or the ACI 318 Appendix D capacity calculations (compared further on in this paper), even though the ACI equation does not consider the influence of lightweight concrete.

It is sometimes difficult to consistently interpret the failure behavior characteristics among the various research studies. For the present review, the definition of a steel or weld failure became subject to closer review and examination. For the pushoff tests, the load-slip characteristics were an important behavior parameter, and, consequently, some researchers conducted deformation-controlled tests to induce a large ultimate slip.

Large inelastic slip deformations will strain the headed studs considerably, such that stud tearing may occur. Although concrete failure defines the first failure mode and the maximum ultimate load, the test result may have been in-

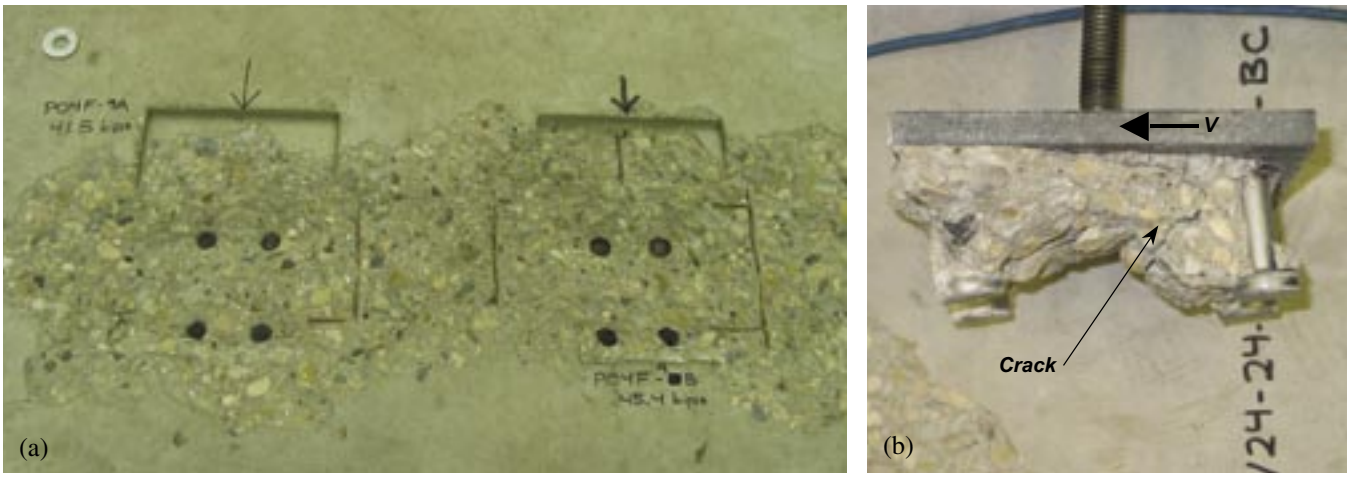

Fig. 10. Failure conditions of Test PO4F-9A and -9B with $y = 4.5$ in. (114 mm): (a) Concrete breakout plan of both tests on slab; (b) Connection plate with concrete intact with crack propagating from front studs to rear.

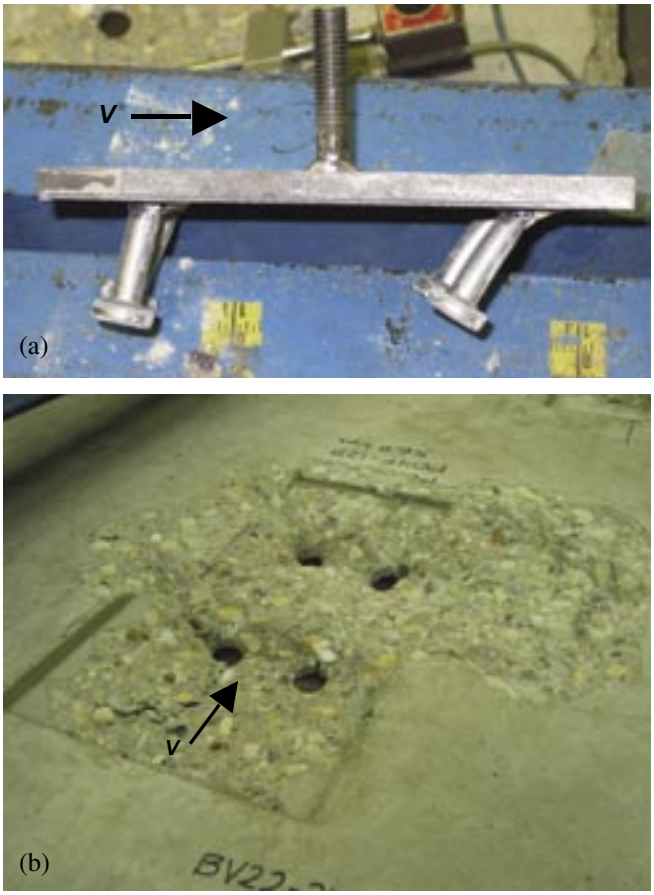

Fig. 11. Failure conditions of Test PO4F-12B with y = 6 in. (152 mm): (a) Deformation of studs after test; (b) Perspective view of the concrete breakout on the slab.

Fig. 12. Mixed mode failure of Test PO4F-12A with y = 6 in. (152 mm) showing steel failure of front studs and concrete breakout at the rear studs.

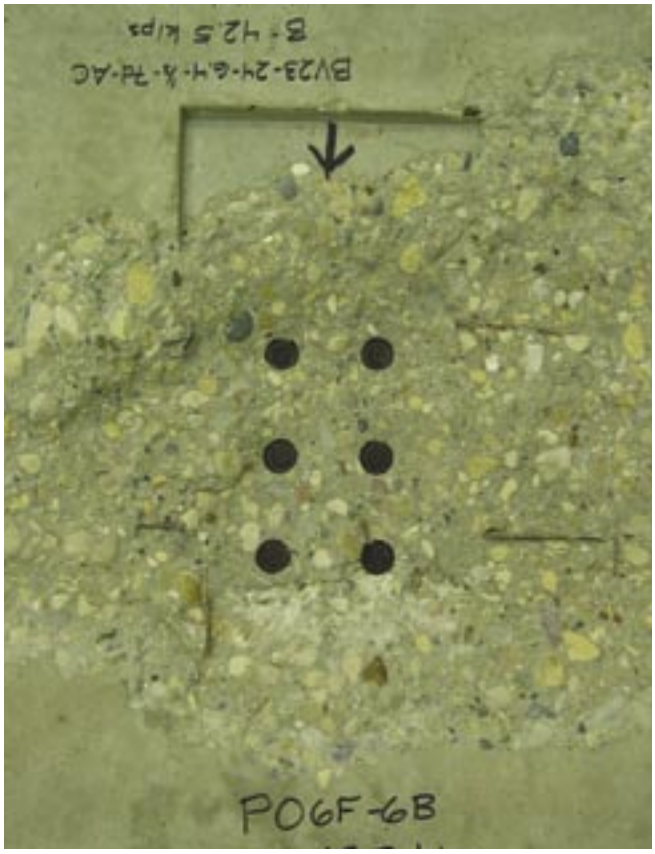

Fig. 13. Breakout plan of six stud Test PO6F-6B with y = 3 in. and Y = 6 in. (76 and 152 mm).

appropriately reported as a steel stud failure, because of the post-failure behavior observed by the researchers. The authors' examination of these test results when compared to a steel failure capacity show that the high slip deformation tests produce an ultimate failure load less than that predicted using $A_s F_{ut}$. This occurred primarily for the short, stocky studs that typically would exhibit pryout behavior.

Eq. (6) is the fractile version of the pryout equation, capped by the steel strength of the studs. The equation includes a spacing modifier, ψ_y, psi, that accounts for influence observed from this database. The database of published results for y-spacing is limited to pushoff tests and four-stud group tests by Zhao,[10] the latter which used a constant y-spacing. This void in the data led the authors to further investigate the y-spacing by conducting tests.

EXPERIMENTAL PROGRAM

As discussed previously, the Zhao[9] and Hawkins[10] tests and the testing from the pushoff literature provide a very extensive database. However, this database is limited to only a few tests examining the influence of y-spacing and the number of y-rows in a connection. Because of this situation, WJE conducted eight pryout tests for the specific purpose of examining the y-spacing influence. The eight tests were included on a slab with other anchorage samples tested as part of a WJE in-house research program.

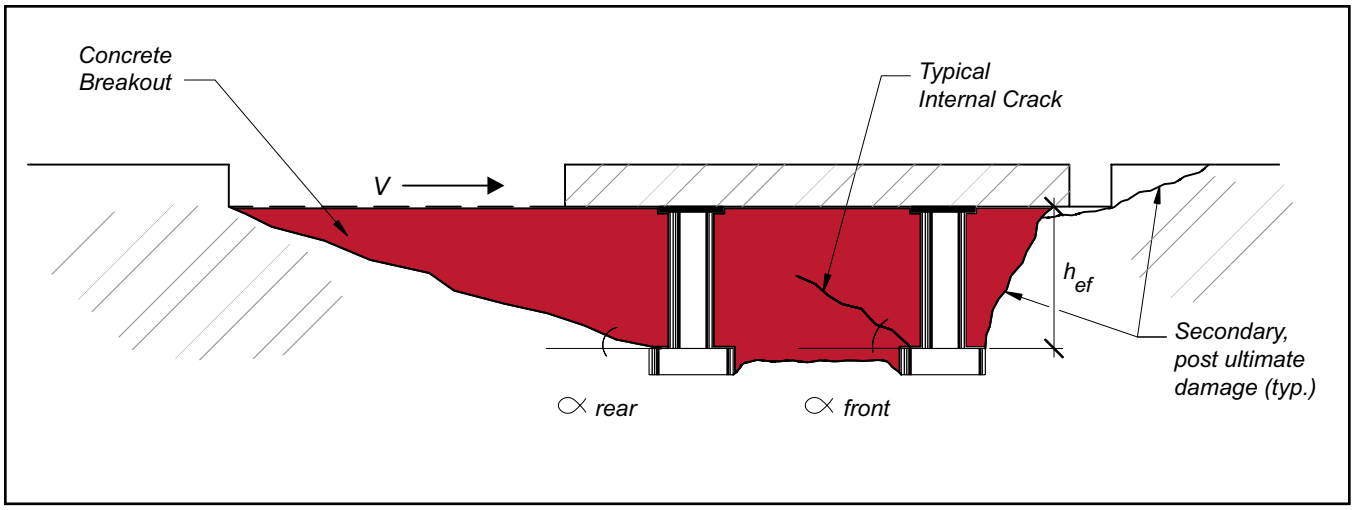

Fig. 14. Typical failure behavior of a pryout connection illustrating the "kick-back" deformation mechanism defining the ultimate failure mode.

Test Specimens

The pryout anchorages were located in the middle of a 5 × 10 × 1.25 ft (1.5 × 3.0 × 0.4 m) deep specimen used for edge testing of connections for another experimental study. The large interior area of this slab permitted tests to be conducted without physically moving the specimen; only the loading apparatus needed to be repositioned. The slab plan is shown in Fig. 6(a).

Fig. 6 shows the eight anchorages tested in this experimental program. All anchorages had a constant *x*-spacing of 3 in. (76.2 mm), which is equivalent to 6*d* for the ½ in. (12.7 mm) studs used. The spacing exceeds the 4*d* requirement of ACI 318 Appendix D. By reviewing the available literature and through discussions with precast producer members, an *x*-spacing of 6*d* was found to be a reasonable spacing to avoid a clustering effect of the studs.

Four anchorage configurations were tested, with two tests conducted per configuration. Six anchorage plate configurations had four studs, with the *y*-spacing varying incrementally from 3 to 6 in. (76.2 to 152 mm). The last test series utilized the overall 6 in. (152 mm) dimension for a *Y*-spacing but placed two additional studs in the center. Thus, the plate had six total studs at an individual *y*-spacing of 3 in. (76.2 mm).

All studs were commercially available nominal 2⅛ in. (54.0 mm) length, with an h_{ef}/d ratio of 3.62. This ratio is less than the 4.5*d* criterion established by Anderson and Meinheit[12] to cause pryout. The Nelson studs used were AWS D1.1 Type B, in conformance with AWS Table 7.1.[36] The studs had

Table 2. Test results for the eight tests from the present test program.

(1)	(2)	(3)	(4)	(5)	(6)	(7)	(8)	(9)	(10)	(11)	(12)	(13)	
Test number	**Number of studs, *n***	**Front row, n_x**	**Side row, n_y**	**Stud diameter, *d* (in.)**	**Embed depth, h_{ef} (in.)**	**Concrete strength, f'_c (psi)**	**Ratio, h_{ef}/d**	**Test geometry**				**V_{steel} (kips)**	
								d_{e3} (in.)	***x*** **(in.)**	***y*** **(in.)**	**Ratio *y/d***		
PO4F-6A	4	2	2	0.5	1.81	5860	3.62	16.5	3.0	3.0	6.0	59.3	
PO4F-6C	4	2	2	0.5	1.81	5920	3.62	16.5	3.0	3.0	6.0	59.3	
PO4F-9A	4	2	2	0.5	1.81	5870	3.62	15.8	3.0	4.5	9.0	59.3	
PO4F-9B	4	2	2	0.5	1.81	5860	3.62	15.8	3.0	4.5	9.0	59.3	
PO4F-12A	4	2	2	0.5	1.81	6230	3.62	39.0	3.0	6.0	12.0	59.3	
PO4F-12B	4	2	2	0.5	1.81	6230	3.62	39.0	3.0	6.0	12.0	59.3	
PO6F-6A	6	2	3	0.5	1.81	6230	3.62	39.0	3.0	3.0	6.0	88.9	
PO6F-6B	6	2	3	0.5	1.81	6230	3.62	39.0	3.0	3.0	6.0	88.9	

Notes:
Column (9): d_{e3} = distance from front stud row to front edge.
Column (15): Pryout mode is a concrete failure mode. Mixed mode is both concrete and steel failure. (Reference Fig. 12.)
Columns (17) to (19): Refer to Fig. 14.
Test data: h = 15 in. (slab thickness); F_{ut} = 75.5 ksi.
1 in. = 25.4 mm; 1 kip = 4.448 kN; 1 psi = 0.006895 MPa; 1 ksi = 6.895 MPa.

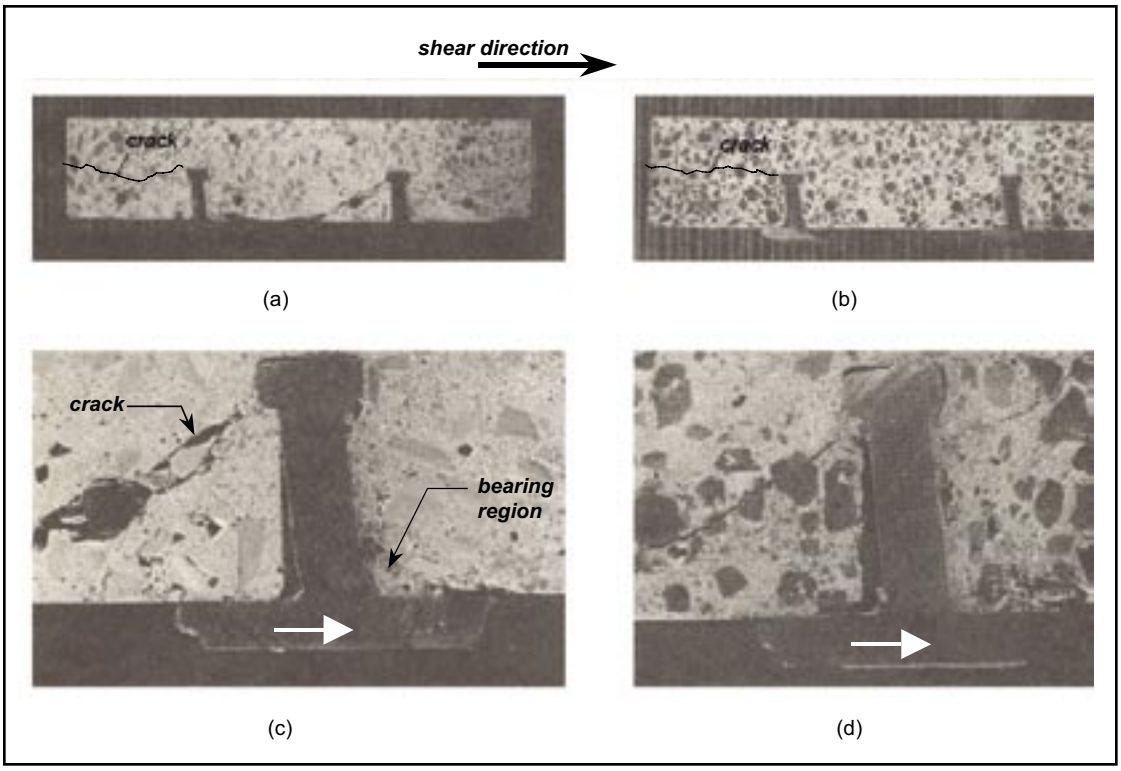

Fig. 15. Splitting cracks in (a) and (b) observed in the rear stud of the pushoff test specimens (from Ollgaard et al.[5]): (a) Normal weight concrete (Specimen LA1); (b) Lightweight concrete (Specimen LE2); (c) Detail of front stud (Specimen LA1); (d) Detail of front stud (Specimen LE2). Note: Splitting cracks in (a) and (b) traced for reproduction purposes.

an actual yield strength of 67.4 ksi (465 MPa) and an ultimate strength of 75.5 ksi (521 MPa). Steel plates were ½ in. (12.7 mm) thick conforming to ASTM A36[37] requirements.

The slab concrete was 5000 psi (34.5 MPa) normal weight concrete containing ½ in. (12.7 mm) angular gravel and no air entrainment. Table 1 shows the material properties for the concrete including compressive strength, splitting tensile strength, and compressive modulus. The slab reached a maximum compressive strength of approximately 6300 psi (43.4 MPa); tests run in this program were conducted when the concrete was in the 5900 to 6300 psi (40.7 to 43.4 MPa) range, which is typical of precast applications.

	(14)	(15)	(16)	(17)	(18)	(19)
	Ultimate V_{test} (kips)	**Failure mode**	**Angle data (degrees)**			
			Computed $\alpha_{front/middle}$	**Measured**		
				α_{front}	α_{middle}	α_{rear}
	43.8	Pryout	31.1	34.5	NA	25.0
	32.6	Pryout	31.1	34.0	NA	29.5
	41.5	Pryout	21.9	35.0	NA	24.0
	45.5	Pryout	21.9	23.5	NA	21.5
	58.2	Mixed	16.8	NA	NA	26.0
	56.8	Pryout	16.8	NA	NA	21.5
	60.1	Pryout	31.1	NA	29.0	26.5
	63.3	Pryout	31.1	NA	35.0	23.5
					Average:	**24.7**

All pryout plates were positioned on the form bottom, with 1 ft 3 in. (381 mm) of concrete placed above. This ensured good consolidation around the headed studs and, thus, trapped air voids were practically eliminated. The slabs were reinforced with a nominal amount of welded wire reinforcement (mesh) for handling purposes; where applicable, the mesh was cut out around the stud anchorages to avoid any possible interference.

To facilitate using a shoe plate test rig in the WJE Jack R. Janney Technical Center laboratory, wood blockouts were installed in front of and behind the anchorage plate. The front blockout prevented the ½ in. (12.7 mm) thick plate from bearing on the concrete and possibly augmenting the shear strength at low load levels.

Testing Procedure

The testing procedure is very similar to that referenced in the Anderson and Meinheit paper.[12] The pryout anchorages were loaded in nearly pure shear by pushing on the back edge of the steel plate to which the headed studs were attached. This load to the embedded plate was achieved by using a ½ in. (12.7 mm) shoe plate welded to a pulling channel, connected to a high strength steel rod inserted through a center hole ram and load cell.

A threaded stud was welded atop each plate, and a nut was finger-tightened on the top to prevent the test fixture and anchorage plate from becoming airborne upon achieving ultimate load. The load was monitored with a load cell, and deformations were recorded with two LVDTs positioned on

the rear side of the plate. The loading fixture and setup is illustrated in Figs. 7 and 8.

Test Behavior and Results

Figs. 9 through 13 show assorted photographs of the eight pryout test failures from this study. All eight tests failed in a concrete failure mode, except Test PO4F-6A, where the two front studs failed in steel and the rear studs failed in a concrete mode. As identified by Zhao,[10] the failure mode and surface were very similar to a tension breakout. However, the failure surface characteristics differed from the overall 35-degree tension concrete breakout mode in that the typical deep failure cone was absent in front of the lead studs.

Figs. 9(a), 10(a), 11(b), and 13 show shallow surface spalling in front of the lead studs. The spalling is post-ultimate, secondary damage. The characteristic breakout from the WJE tests is shown in Fig. 14. All failures were somewhat explosive at ultimate load.

In general, when the anchorage plates were removed from the slab, the concrete enclosed by the studs was typically intact and confined within the stud perimeter; this is illustrated in Figs. 9(b) and 10(b). Observations of a number of the intact pieces of confined concrete within the studs, not damaged by post-failure autopsies, revealed an interesting cracking behavior that typically occurred behind the front studs.

The large front stud shank deformation at the plate relative to the embedded stud heads caused a diagonal crack to initiate at the head and propagate diagonally upward at an angle of approximately 35 degrees until intersecting the plate underside [see Figs. 9(b) and 10(b) for crack location]. Under load, this triangular concrete wedge behind the front studs was thus well confined, especially along the top edge (see Fig. 14).

A similar behavior was observed at the rear studs. However, the concrete free surface is not confined by a plate behind the rear studs, and this diagonal crack propagation and wedge development eventually lead to defining the concrete breakout surface. This "kick-back" action or prying out of the concrete defines this unique failure mode characteristic. This behavior was reported and illustrated in the work of Ollgaard et al. (see Fig. 15).[5] However, the failure mode was mislabeled as a concrete failure instead of a pryout failure.

Table 2 presents the test results with their associated concrete strengths and failure loads. Also included in this table is a predictor of the steel strength in shear. Review of the failure loads in Table 2 reveals an increase in failure load for a corresponding increase in *y*-spacing. For the four-stud group tests, represented by the Series PO4F-6_ (y = 3 in.), PO4F-9_ (y = 4½ in.), and PO4F-12_ (y = 6 in.), the increase in load is not directly proportional to *y*-spacing.

For example, the average failure load for Series PO4F-12_ is not twice the average failure load of Series PO4F-6_, even though the *y*-spacing increased from 3 to 6 in. (76.2 to 152 mm). Fig. 16 is a plot of the normalized failure load versus the overall *Y*-spacing for the eight tests shown in Table 2.

Series PO4F-12_ and PO6F-6_ were

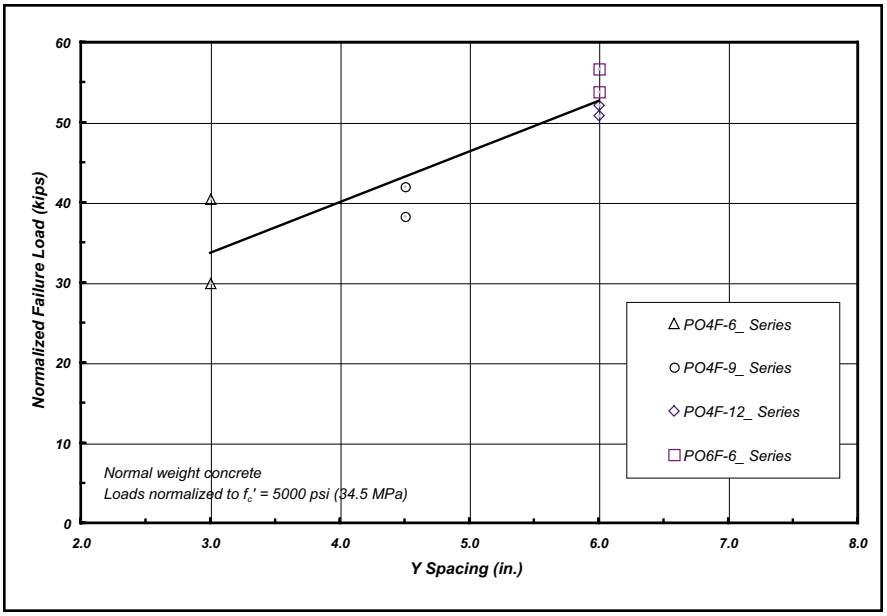

Fig. 16. Normalized failure load versus the overall *Y*-spacing for the eight tests of the present study.

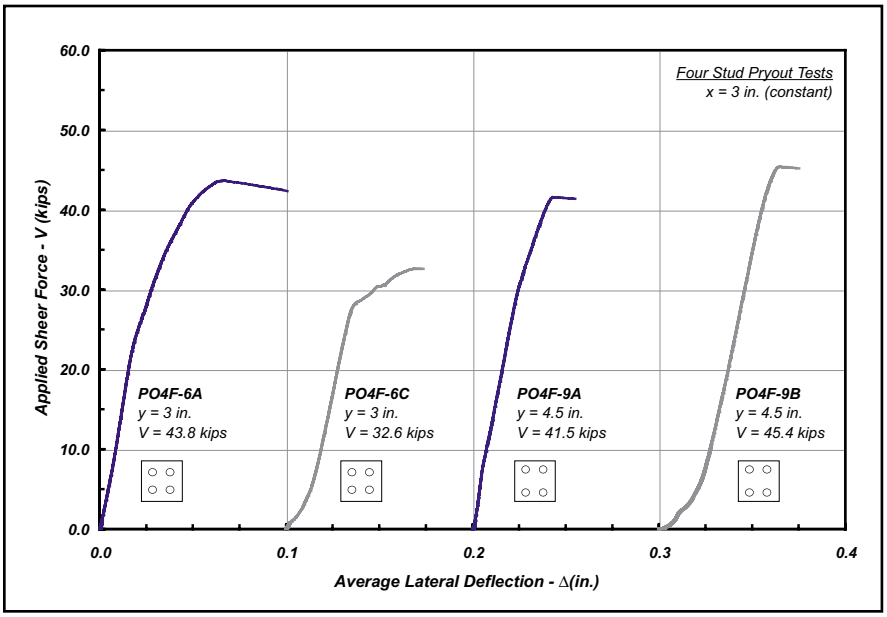

Fig. 17. Load-deflection curves for the four-stud pryout tests with y = 3 and 4.5 in. (76.2 and 114 mm).

similar in that the out-to-out or overall, center-to-center *Y*-spacing (where $Y = \Sigma y$) was 6 in. (152 mm). Series PO6F-6_ had an additional *y*-row of two studs placed in the anchorage plate center, giving a total of six studs in the anchorage. The two additional studs in Series PO6F-6_ provided only a slight increase in failure load over the four-stud anchorages of Series PO4F-12_.

This indicates that the overall *Y*-spacing is the more influential parameter governing the behavior, yet the interior studs provide a "disruption" to the concrete stress state below the plate that minimizes the added benefit of the additional studs. Therefore, the individual *y*-spacing present in the connection is an influential parameter in that it defines the overall anchorage capacity.

The load-deflection behavior of the eight tests is shown in Figs. 17 and 18. Series PO4F-6_ and PO4F-9_ showed fairly stiff, linear behavior under increased load until their sudden and explosive failure. Series PO4F-12_ showed good ductile behavior up until failure.

Test PO4F-12A was a mixed mode failure, whereas Test PO4F-12B was a concrete failure with shear tearing of the studs observed on the removed anchorage plate. As illustrated in Fig. 18, Tests PO6F-6A and PO6F-6B showed similar load-deflection behavior as their companion four-stud tests, but their initial slope was less, and the failure mode is characterized as more brittle.

DATA ANALYSIS FOR *y*-SPACING

The experimental results from the work herein and research studies of Hawkins,[9] Zhao,[10] and numerous composite pushoff testing programs reported in the literature were collected into a *y*-spacing database of 82 total tests. The test database consists of the present eight tests along with nine tests from Zhao. The remaining 65 tests were multiple *y*-row pushoff tests reported in the literature.

Of the pushoff tests, 27 tests were in lightweight aggregate concrete for which an appropriate λ factor was employed. Because Eq. (5) showed reasonable correlation with lightweight concrete results when there was a single *y*-row, the lightweight and normal weight concrete tests were combined in the *y*-spacing analysis and not partitioned separately. Furthermore, the database size would have been too restrictive by separating these variables.

Fig. 19 shows the test-to-predicted capacity ratio versus *y*/*d* spacing ratio for the multiple *y*-row tests. The single anchor predicted capacity is based on Eq. (5). The database values represented in this plot have *y*/*d* ratios ranging from 2.1 to about 20. The plot shows a curvilinear trend to the data, with both the conventional pryout tests and pushoff tests following the same general trend. Using a multi-variable, linear regression analysis on this *y*-spacing data, the following factor was found to account for the influence of *y*-spacing:

$$\psi_y = \frac{\sqrt{y}}{4d} \tag{8}$$

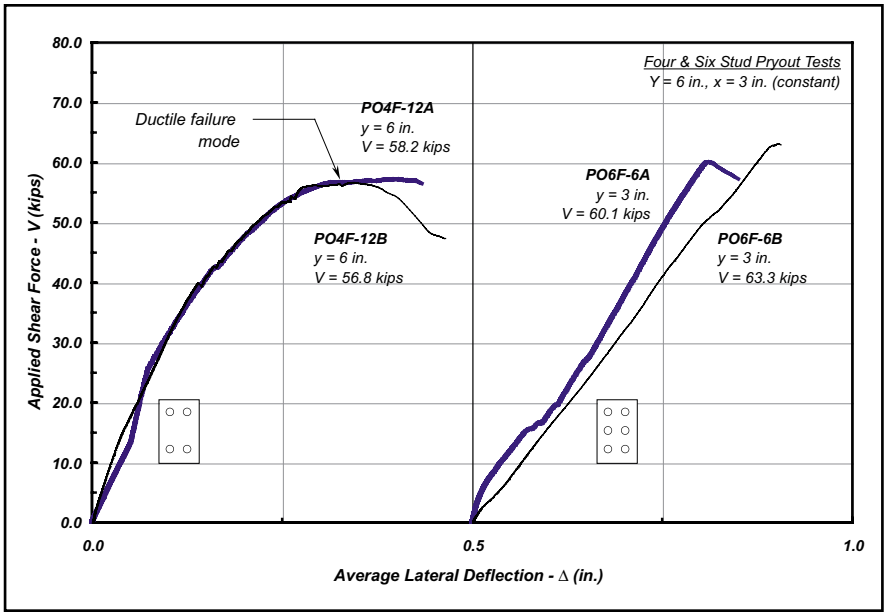

Fig. 18. Load-deflection curves for the four- and six-stud pryout tests with $Y = 6$ in. (152 mm).

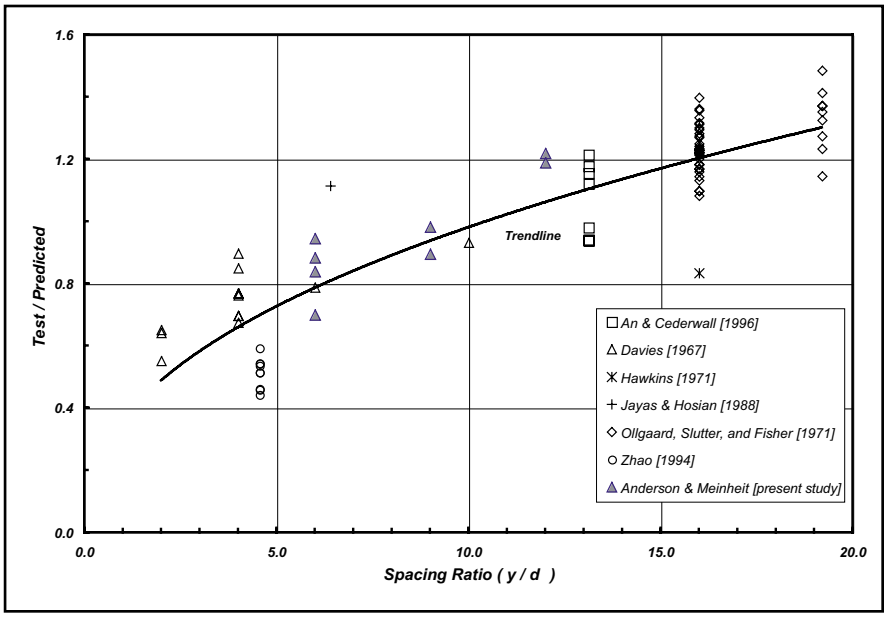

Fig. 19. Test-to-predicted capacity using Eq. (5) versus spacing ratio (*y*/*d*) for the multiple *y*-row pushoff and pryout tests.

where

ψ_y = y-spacing factor between rows perpendicular to applied shear force for $y/d \le 20$

y = individual, center-to-center spacing of anchor rows in Cartesian y-direction (in.)

d = stud diameter (in.)

The statistical parameters when evaluating the y-spacing database alone gave a prediction mean of 1.00, a standard deviation of 0.12, and a COV of 12.1 percent. The statistics show that there is good correlation of the data with this factor considering that about one-third of the database includes lightweight aggregate concrete tests. The filled triangular shaped data points in Fig. 19 represent the tests of the present study, and these data track well with the entire multiple y-row database.

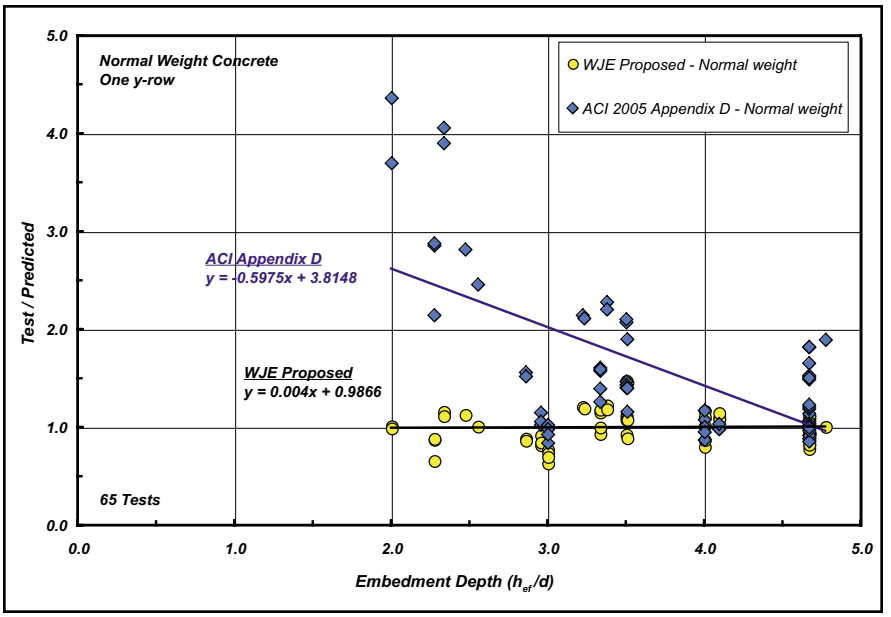

Fig. 20. Test-to-predicted capacity versus embedment depth ratio (h_{ef}/d) for normal weight concrete, one y-row tests comparing the average equations from ACI 318-05 Appendix D and the proposed Eq. (5).

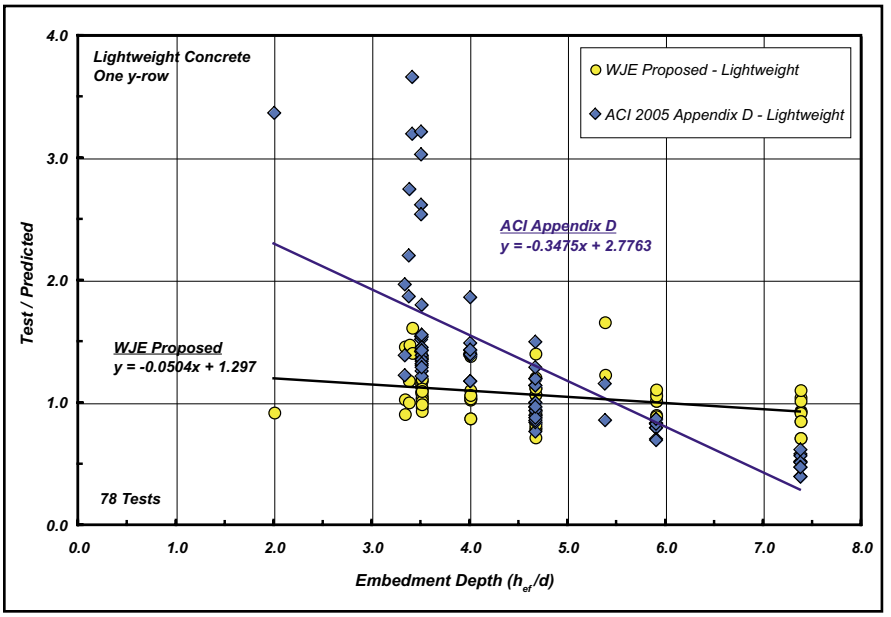

Fig. 21. Test-to-predicted capacity versus embedment depth ratio (h_{ef}/d) for lightweight concrete, one y-row tests comparing the average equations from ACI 318-05 Appendix D and the proposed Eq. (5).

COMPARISON TO ACI 318-05 REQUIREMENTS

As discussed at the beginning of this paper, the ACI 318-05 Appendix D[1] concrete breakout capacity for the pryout failure mode requires the calculation of the tensile breakout capacity based on computing the effective area of the CCD physical model breakout surface, and modifying that capacity by k_{cp}, a step function term that is correlated with embedment depth.

Figs. 20 through 23 present test-to-predicted capacity versus embedment depth ratio (h_{ef}/d) plots for one y-row in normal weight concrete, one y-row in lightweight concrete, multiple y-rows in both concrete types, and all data, respectively. The plots provide comparisons of the average predictor equations from ACI and that proposed herein as average Eq. (5), modified by the Eq. (8) y-spacing factor, as required. For reference, the ACI 318 Appendix D equation uses a 5 percent fractile design equation for the tensile breakout strength in the pryout capacity equation, given by:

$$N_{cbg} = 24\sqrt{f'_c}\,(h_{ef})^{1.5}\left(\frac{A_N}{A_{No}}\,\psi_1\psi_2\psi_3\right) \quad (9)$$

The unreduced average equation corresponding to the above concrete tensile breakout for uncracked concrete is given by Eq. (10):[13]

$$N_{cbg} = 40\sqrt{f'_c}\,(h_{ef})^{1.5}\left(\frac{A_N}{A_{No}}\,\psi_1\psi_2\right) \quad (10)$$

where $\psi_1 = \psi_2 = 1.0$.

For the portioned databases shown in Figs. 20 to 22, it can be observed that the ACI 318 Appendix D average predictor equations using Eq. (10) are overly conservative for short stocky studs where pryout is likely to occur. For deeper embedded studs, the ACI design approach becomes unconservative.

When the entire database of single and multiple y-row pushoff and pryout tests are evaluated with the ACI 318 Appendix D procedure, the ACI predicted results are clearly overly conservative for headed studs, as depicted in Fig. 23. The inherent conservatism of the ACI equation occurs when the k_{cp} factor becomes 1.0, as shown on the

left side of Fig. 23; several data points are located above the test/predicted ratio of 2.0.

If the entire 225 test database is compared to the prediction of capacity calculated using Eqs. (5) and (8), the prediction mean is 1.02, the standard deviation is 0.164, and the COV is 16.1 percent. By comparison, the ACI 318 Appendix D statistics are not near as good and exhibit considerable scatter. For the ACI average equations, the prediction mean is 2.03, the standard deviation is 1.205, and the COV is 60 percent.

From Figs. 21 to 23 and the above statistical summaries, the average ACI 318 Appendix D provisions for pryout under-predict the true capacity of a pryout anchorage. Representing pryout behavior with an easily illustrative, physical behavioral model is admirable, but the above analyses show the unnecessarily conservative limitations in the ACI method of predicting pryout capacity.

CONCLUSIONS AND DESIGN RECOMMENDATIONS

Based on this study, the following conclusions and recommendations are offered:

1. Headed studs in normal weight concrete with a h_{ef}/d less than 4.5 may invoke a failure mode known as pryout. This failure mode produces an ultimate capacity less than that predicted by Eq. (1), that is, $V_u = 1.0\, nA_s F_{ut(design)}$.

2. When headed studs are embedded in lightweight aggregate concrete, the h_{ef}/d limit is not as well defined because of the nature of lightweight aggregate concrete. From the literature, it was found that this ratio varies from about 5.4 to 7.4.

3. Eqs. (6), (7), and (8) are proposed to predict the capacity for short, stocky studs having h_{ef}/d ratios less than 4.5.

4. Proposed Eqs. (6), (7), and (8) provide good correlation to predicting the pryout capacity. The equations are based on a database of 225 tests, presented in Appendix B of this paper.

5. The ACI 318-05 Appendix D provisions for predicting pryout capacity are overly conservative and reflect poor prediction statistics. The ACI model, based on a pseudo-tension breakout, is not appropriate for predicting pryout capacity.

RESEARCH NEEDS

Although the database presented in Appendix B is a substantial one, it is still primarily dominated by pushoff data. The pryout tests conducted as part of this study show ultimate load behavior and predictive statistics in line with the pushoff tests. Additional work is recommended to study the influence of shear lag when a greater *y*-spacing exists.

ACKNOWLEDGMENTS

Wiss, Janney, Elstner Associates, Inc., would like to express its gratitude to the Precast/Prestressed Concrete Institute for sponsoring this comprehensive research program on headed studs.

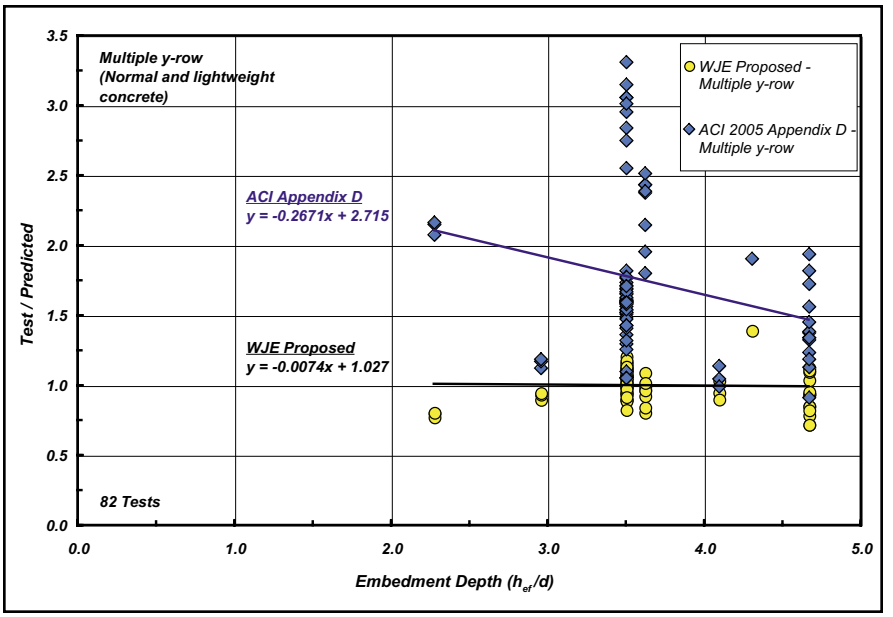

Fig. 22. Test-to-predicted capacity versus embedment depth ratio (h_{ef}/d) for multiple *y*-row tests comparing the average equations from ACI 318-05 Appendix D and the proposed Eq. (5).

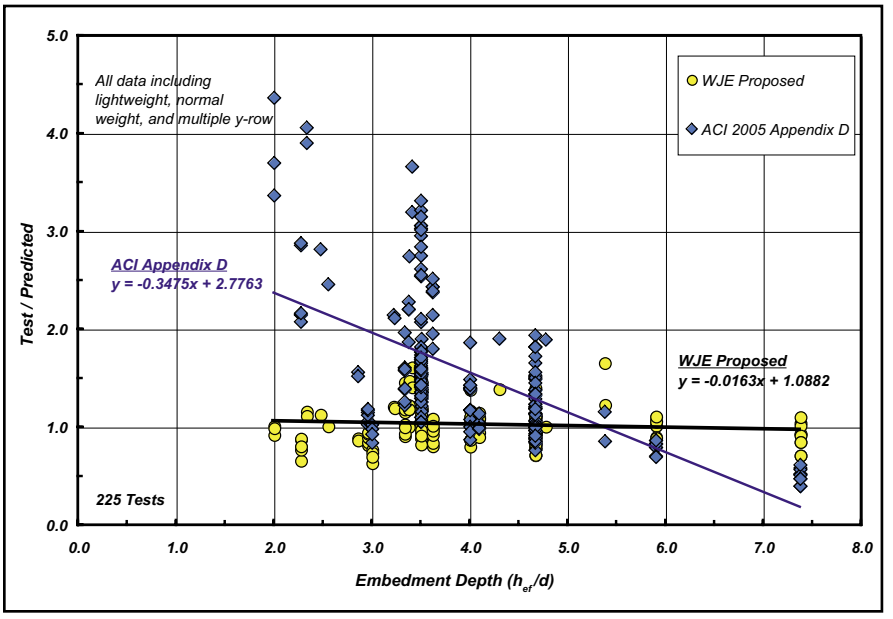

Fig. 23. Test-to-predicted capacity versus embedment depth ratio (h_{ef}/d) for all test data comparing the average equations from ACI 318-05 Appendix D and the proposed Eq. (5).

WJE also expresses its appreciation to Harry Chambers, Don Sues, and Donald Merker of Nelson Stud Welding for their contributions of technical training, stud material donation, stud welding services, and additional laboratory support in Ohio. Gratitude is expressed to Roger Becker, vice president of Spancrete Industries in Waukesha, Wisconsin, and that entire organization for their accurate fabrication and donation of the slab for this study. Both companies are commended for their respective contributions to practical research for the precast concrete industry.

The authors wish to thank their employer, Wiss, Janney, Elstner Associates, Inc., for having the foresight and dedicating the resources in sponsoring in-house research such as this so the anchorage conditions reported herein could be investigated, tested, and reported to the structural engineering community.

Publications cited in the literature were oftentimes difficult to locate, especially the pushoff literature and reports from the 1960s. Special thanks is extended to Dr. James Baldwin, Civil Engineering Professor Emeritus, University of Missouri-Columbia for locating and loaning WJE numerous out-of-print University of Missouri research reports and engineering experimental station bulletins. Other literature was located through the hard work and persistence of Penny Sympson, WJE Corporate Librarian, and her efforts were invaluable to this work.

The thoughtful and constructive review comments and suggestions from the PCI JOURNAL manuscript reviewers are acknowledged and appreciated.

REFERENCES

1. ACI Committee 318, "Building Code Requirements for Structural Concrete (ACI 318-05) and Commentary (ACI 318R-05)," American Concrete Institute, Farmington Hills, MI, 2005.
2. PCI Committee on Precast Sandwich Wall Panels, "State-of-the-Art of Precast/Prestressed Sandwich Wall Panels," PCI JOURNAL, V. 42, No. 2, March-April 1997, pp. 92-134.
3. AISC, *Manual of Steel Construction: Allowable Stress Design,* Ninth Edition, American Institute of Steel Construction, Chicago, IL, 1989.
4. AISC, *Manual of Steel Construction: Load & Resistance Factor Design (LRFD)*, V. I (Structural Members, Specifications & Codes), Third Edition, American Institute of Steel Construction, Chicago, IL, 2001.
5. Ollgaard, J. G., Slutter, R. G., and Fisher, J. W., "Shear Strength of Stud Connectors in Lightweight and Normal-Weight Concrete," *AISC Engineering Journal*, V. 8, No. 2, April 1971, pp. 55-64.
6. Shaikh, A. F., and Yi, W., "In Place Strength of Welded Headed Studs," PCI JOURNAL, V. 30, No. 2, March-April 1985, pp. 56-81.
7. *PCI Design Handbook: Precast and Prestressed Concrete*, Third Edition, Precast/Prestressed Concrete Institute, Chicago, IL, 1985.
8. *PCI Design Handbook: Precast and Prestressed Concrete*, Fourth Edition, Precast/Prestressed Concrete Institute, Chicago, IL, 1992.
9. Hawkins, N., "Strength in Shear and Tension of Cast-in-Place Anchor Bolts," *Anchorage to Concrete*, SP-103, American Concrete Institute, Detroit, MI, 1987, pp. 233-255.
10. Zhao, G., "Tragverhalten von randfernen Kopfbolzenverankerungen bei Betonbruch (Load-Carrying Behavior of Headed Stud Anchors in Concrete Breakout Away From an Edge)," Report 1994/1, Institut für Werkstoffe im Bauwesen, Universität of Stuttgart, Stuttgart, Germany, 1994, 197 pp. [in German].
11. Anderson, N. S., and Meinheit, D. F., "Design Criteria for Headed Stud Groups in Shear: Part 1—Steel Capacity and Back Edge Effects," PCI JOURNAL, V. 45, No. 5, September-October 2000, pp. 46-75.
12. Anderson, N. S., and Meinheit, D. F., "Steel Capacity of Headed Studs Loaded in Shear," *Proceedings (PRO 21)*, RILEM Symposium on Connections Between Steel and Concrete, University of Stuttgart, Germany (10-12 September 2001), Edited by R. Eligehausen, 2001, RILEM Publications S.A.R.L., Cachan, France, pp. 202-211.
13. Fuchs, W., Eligehausen, R., and Breen, J. E., "Concrete Capacity Design (CCD) Approach for Fastening to Concrete," *ACI Structural Journal*, V. 92, No. 1, January-February 1995, pp. 73-94.
14. Viest, I. M., "Investigation of Stud Shear Connectors for Composite Concrete and Steel T-Beams," *Journal of the American Concrete Institute*, V. 27, No. 8, April 1956, pp. 875-891.
15. Driscoll, G. C., and Slutter, R. G., "Research on Composite Design at Lehigh University," *Proceedings of the National Engineering Conference*, American Institute of Steel Construction, May 1961, pp. 18-24.
16. Baldwin, Jr., J. W., Henry, J. R., and Sweeney, G. M., "Study of Composite Bridge Stringers—Phase II," *Technical Report*, University of Missouri-Columbia, Department of Civil Engineering, Columbia, MO, May 1965, 113 pp.
17. Baldwin, Jr., J. W., "Composite Bridge Stringers—Final Report," *Report 69-4,* Missouri Cooperative Highway Research Program, Missouri State Highway Department and University of Missouri-Columbia, Columbia, MO, May 1970, 62 pp.
18. Buttry, K. E., "Behavior of Stud Shear Connectors in Lightweight and Normal-Weight Concrete," *Report 68-6,* Missouri Cooperative Highway Research Program, Missouri State Highway Department and University of Missouri-Columbia, Columbia, MO, August 1965, 45 pp.
19. Dallam, L. N., "Design of Shear Connectors in Composite Concrete-Steel Bridges," *Report 67-7,* Missouri Cooperative Highway Research Program, Missouri State Highway Department and University of Missouri-Columbia, Columbia, MO, 1967, 20 pp.
20. Dallam, L. N., "Push-Out Tests of Stud and Channel Shear Connectors in Normal-Weight and Lightweight Concrete Slabs," *Bulletin Series No. 66,* Engineering Experiment Station Bulletin, University of Missouri-Columbia, Columbia, MO, April 1968, 76 pp.
21. Goble, G. G., "Shear Strength of Thin Flange Composite Specimens," *Engineering Journal,* American Institute of Steel Construction, V. 5, No. 2, April 1968, pp. 62-65.
22. Dhir, T. J., "Use of Stud Shear Connectors in Composite Construction," MS Thesis, University of Colorado, Boulder, CO, May 1964, 110 pp.
23. Steele, D. H., "The Use of Nelson Studs with Lightweight Aggregate Concrete in Composite Construction," MS Thesis, University of Colorado, Boulder, CO, October 1967, 143 pp.
24. Chinn, J., "Pushout Tests on Lightweight Composite Slabs," *AISC Engineering Journal*, V. 2, No. 4, October 1965, pp. 129-134.
25. Davies, C., "Small-Scale Push-out Tests on Welded Stud Shear Connectors," *Concrete*, V. 1, No. 9, September 1967, pp. 311-316.
26. Hawkins, N. M., "The Strength of Stud Shear Connectors," *Research Report No. R141*, Department of Civil Engineering,

University of Sydney, Sydney, Australia, December 1971, 34 pp.
27. Oehlers, D. J., "Splitting Induced by Shear Connectors in Composite Beams," *Journal of Structural Engineering*, American Society of Civil Engineers, V. 115, No. 2, February 1989, pp. 341-362.
28. Oehlers, D. J., and Park, S. M., "Shear Connectors in Composite Beams with Longitudinally Cracked Slabs," *Journal of Structural Engineering*, American Society of Civil Engineers, V. 118, No. 8, August 1992, pp. 2004-2022.
29. Kulak, G. L., Fisher, J. W., and Struik, J. H. A., *Guide to Design Criteria for Bolted and Riveted Joints*, Second Edition, John Wiley and Sons, New York, NY, 1987, 333 pp.
30. *PCI Design Handbook: Precast and Prestressed Concrete*, Second Edition, Precast/Prestressed Concrete Institute, Chicago, IL, 1978.
31. AISC, *Manual of Steel Construction,* Eighth Edition, American Institute of Steel Construction, Chicago, IL, 1980.
32. ICBO, *Uniform Building Code,* 1979 Edition, International Conference of Building Officials, Whittier, CA, 1979.
33. ASTM, *Standard Specification for Structural Bolts, Steel, Heat Treated, 120/105 ksi Minimum Tensile Strength* (ASTM A325-04), V. 01.08, 2004, American Society for Testing and Materials, West Conshohocken, PA, 2004.
34. AASHO, *Standard Specifications for Highway Bridges*, Eighth Edition, American Association of State Highway Officials, Washington, DC, 1961.
35. Wollmershauser, R. E., "Anchor Performance and the 5% Fractile," *Hilti Technical Services Bulletin*, Hilti, Inc., Tulsa, OK, November 1997, 5 pp.
36. AWS, *Structural Welding Code – Steel*, AWS D1.1 / D1.1M: 2004, 19th Edition, American Welding Society, Miami, FL, 2004.
37. ASTM, *Standard Specification for Carbon Structural Steel* (ASTM A36/A36M-03a), V. 01.04, 2003, American Society for Testing and Materials, West Conshohocken, PA, 2003.
38. Hawkins, N. M., and Mitchell, D., "Seismic Response of Composite Shear Connections," *Journal of Structural Engineering*, American Society of Civil Engineers, V. 110, No. 9, September 1984, pp. 2120-2136.
39. An, L., and Cederwall, K., "Push-out Tests on Studs in High Strength and Normal Strength Concrete," *Journal of Constructional Steel Research*, V. 36, No. 1, 1996, pp. 15-29.
40. Jayas, B. S., and Hosain, M. U., "Behavior of Headed Studs in Composite Beams: Push-out Tests," *Canadian Journal of Civil Engineering*, V. 15, No. 2, April 1988, pp. 240-253.

APPENDIX A – NOTATION

A_s = effective cross-sectional area of stud anchor, sq in.
A_{se} = effective cross-sectional area of stud anchor, sq in. (ACI 318-05 Appendix D notation)
d = shaft diameter of headed stud, in.
d_{e1} = side edge distance normal to shear load application direction, parallel to the x-axis, taken from the center of an anchor shaft to the side concrete edge, in.
d_{e2} = side edge distance normal to shear load application direction, parallel to the x-axis, taken from the center of an anchor shaft to the side concrete edge, in. (d_{e2} is the side edge distance opposite d_{e1})
d_{e3} = front edge distance parallel to shear load application direction and y-axis, taken from the center of a front anchor shaft to the front concrete edge, in.
d_{e4} = back or rear edge distance parallel to shear load application direction and y-axis, taken from the center of a back anchor shaft to the rear concrete edge, in.
E_c = modulus of elasticity of concrete, psi
f'_c = specified compressive strength of concrete, psi
$F_{ut\,(actual)}$ = actual ultimate tensile strength of headed stud steel in tension, psi
$F_{ut\,(design)}$ = design minimum tensile strength of headed stud steel in tension, psi
F_{ut}, f_{ut} = specified ultimate tensile strength of anchor steel in tension, psi
F_{vy} = shear yield strength of anchor steel, psi
F_y, f_y = specified yield strength of anchor steel in tension, psi
h = thickness of a concrete member in which the anchors are embedded, measured parallel to the anchor axis, in.
h_{ef} = effective headed stud embedment depth taken as the length under the head to the concrete surface, in.
k_{cp} = coefficient for pryout strength (from ACI 318-05 Appendix D)
L = overall length in the y-direction between the outermost anchors in a connection = Σy, in. (from AISC)
n = number of anchors in a connection or group
N_{cb} = nominal concrete breakout strength in tension of a single anchor, lb (from ACI 318-05 Appendix D)
Q = nominal strength of a stud shear connector embedded in a solid concrete slab, lb (from AISC)
t = thickness of the attachment plate, in.
t_f = flange thickness of a structural steel shape, in.
V_{cp} = nominal concrete pryout strength, lb (from ACI 318-05 Appendix D)
V_n = nominal shear strength, lb
V_s, V_{steel} = nominal shear strength of a single headed stud or group of headed studs governed by steel strength, lb
x = center-to-center spacing of stud anchors in the x direction of the Cartesian plane, in.
x = eccentricity between the shear plane and centroidial axis of the connected component, in. (from AISC)
y = center-to-center spacing of stud anchors in the y direction of the Cartesian plane, in.
λ = concrete unit weight factor
= 1.0 for normal weight concrete
= 0.85 for sand lightweight concrete
= 0.75 for all lightweight concrete
$\varkappa$ = one-sided population limit (fractile) factor for a normal distribution
μ = coefficient of friction
ϕ = strength reduction factor
ψ_y = y-spacing factor

APPENDIX B – DATABASE TEST RESULTS

(1)	(2)	(3)	(4)	(5)	(6)	(7)	(8)	(9)	(10)	(11)	(12)	(13)	(14)	(15)	(16)	(17)	(18)	(19)	(20)	(21)	(22)	(23)	(24)	(25)	(26)
Investigators	**Test number**	**No. of studs, n**	**Front row (FR)**	**Back row (BR)**	**Side row (SR)**	**Stud dia., d (in.)**	**Embed depth, h_{ef} (in.)**	**Concrete strength, f'_c (psi)**	**Concrete modulus, E_c (ksi)**	**Concrete splitting strength, f_{sp} (psi)**	**Concrete density, w_c (lb/ft³)**	**LW factor, λ**	**h_{ef}/d**	**Test geometry**				**1 side V test (kips)**	**Stud strength, F_u (ksi)**	**Steel ratio, Test / Pred**	**Report failure mode**	**$V_{poc} = V_{po} * \psi_y$ (kips)**	**Test / Pred**	**ACI V_{cp} (kips)**	**Test / Pred**
														d_{c3} (in.)	x (in.)	y (in.)	h (in.)								
Lightweight Concrete - Single Y Row																									
Buttry[18]	L6B4A2	2	2	0	1	0.750	1.50	4590	1775	370	85.8	0.81	2.00	13.0	4.0	0.0	6.0	25.8	62.1	0.47	Pull-out	27.9	0.92	7.66	3.37
Buttry[18]	L6B4A3	2	2	0	1	0.750	2.50	3570	1870	326	96.6	0.81	3.33	13.0	4.0	0.0	6.0	32.8	62.1	0.60	Concrete	31.8	1.03	23.59	1.39
Buttry[18]	L6B4B3	2	2	0	1	0.750	2.50	5040	1980	387	89.4	0.81	3.33	13.0	4.0	0.0	6.0	34.4	62.1	0.63	Concrete	37.7	0.91	28.03	1.23
Dhir[22] and Chinn[24]	6BI 3-3	2	2	0	1	0.750	2.50	4870	2381	NR	93	0.75	3.33	8.0	4.0	0.0	6.0	50.0	72.1	0.78	Stud	34.2	1.46	25.38	1.97
Buttry[18]	L4B4A2	2	2	0	1	0.500	1.69	4260	1900	356	92.0	0.81	3.38	13.0	4.0	0.0	6.0	18.4	75.5	0.62	Stud	15.5	1.19	8.34	2.21
Buttry[18]	L4B4B2	2	2	0	1	0.500	1.69	4580	2040	369	94.2	0.81	3.38	13.0	4.0	0.0	6.0	16.2	75.5	0.55	Weld	16.1	1.01	8.65	1.87
Dhir[22] and Chinn[24]	4BI 1-2	2	2	0	1	0.500	1.69	5485	2392	NR	93	0.75	3.38	8.0	4.0	0.0	6.0	24.0	71.2	0.86	Stud	16.2	1.48	8.73	2.75
Dhir[22] and Chinn[24]	5BI 1-2 5/8	2	2	0	1	0.625	2.13	4910	2299	NR	93	0.75	3.41	8.0	4.0	0.0	6.0	34.0	68.8	0.81	Stud	24.1	1.41	10.63	3.20
Dhir[22] and Chinn[24]	5BI 2-2 5/8	2	2	0	1	0.625	2.13	4200	2404	NR	93	0.75	3.41	8.0	4.0	0.0	6.0	36.0	68.8	0.85	Stud	22.3	1.62	9.83	3.66
Baldwin[17]	L5B4E2.5	2	2	0	1	0.625	2.19	3000	1960	NR	105.6	0.85	3.50	13.0	4.0	0.0	6.0	29.4	64.2	0.75	Concrete	21.6	1.36	9.70	3.03
Baldwin[17]	L5B4F2.5	2	2	0	1	0.625	2.19	3000	1960	NR	105.6	0.85	3.50	13.0	4.0	0.0	6.0	31.2	64.2	0.79	Concrete	21.6	1.44	9.70	3.22
Buttry[18]	L5B4H2.5	2	2	0	1	0.625	2.19	4030	1850	346	92.1	0.81	3.50	13.0	4.0	0.0	6.0	28.2	64.2	0.72	Concrete	24.0	1.17	10.77	2.62
Buttry[18]	L5H4A2.5	2	2	0	1	0.625	2.19	3440	1825	296	96.2	0.75	3.50	13.0	4.0	0.0	6.0	23.4	64.2	0.59	Pull-out	20.5	1.14	9.20	2.54
Ollgaard et al.[5]	2E(1)	2	2	0	1	0.750	2.63	4400	2210	390	111.1	0.88	3.50	14.0	4.0	0.0	6.0	42.4	70.9	0.68	Stud	38.9	1.09	29.86	1.42
Ollgaard et al.[5]	2E(2)	2	2	0	1	0.750	2.63	4400	2210	390	111.1	0.88	3.50	14.0	4.0	0.0	6.0	46.2	70.9	0.74	Stud	38.9	1.19	29.86	1.55
Ollgaard et al.[5]	2E(3)	2	2	0	1	0.750	2.63	4400	2210	390	111.1	0.88	3.50	14.0	4.0	0.0	6.0	45.4	70.9	0.72	Stud	38.9	1.17	29.86	1.52
Steele[23]	37-A	2	2	2	1	0.749	2.625	3790	1574	292	84.4	0.75	3.50	8.0	4.0	0.0	6.0	36.5	76.2	0.54	Concrete	30.8	1.18	23.69	1.54
Steele[23]	40-A	2	2	2	1	0.749	2.625	3545	1690	306	90.5	0.77	3.50	8.0	4.0	0.0	6.0	36.5	76.2	0.54	Concrete	30.5	1.20	23.43	1.56
Steele[23]	31-A	2	2	2	1	0.749	2.625	3240	1883	301	100.2	0.79	3.50	8.0	4.0	0.0	6.0	33.0	76.2	0.49	Concrete	30.0	1.10	23.05	1.43
Steele[23]	42-A	2	2	2	1	0.749	2.625	3730	1839	324	94.1	0.79	3.50	8.0	4.0	0.0	6.0	32.5	76.2	0.48	Concrete	32.3	1.01	24.81	1.31
Steele[23]	36-C-1	2	2	2	1	0.749	2.625	4380	2026	365	95.1	0.82	3.50	8.0	4.0	0.0	6.0	38.0	76.2	0.57	Concrete	36.4	1.04	27.95	1.36
Steele[23]	30-A	2	2	2	1	0.749	2.625	3420	1523	329	85.4	0.84	3.50	8.0	4.0	0.0	6.0	35.0	76.2	0.52	Concrete	32.8	1.07	25.19	1.39
Steele[23]	31-B-2	2	2	2	1	0.749	2.625	3770	2520	358	115.7	0.87	3.50	8.0	4.0	0.0	6.0	36.8	76.2	0.55	Concrete	35.7	1.03	27.41	1.34
Steele[23]	42-B	2	2	2	1	0.749	2.625	2985	1562	330	90.9	0.90	3.50	8.0	4.0	0.0	6.0	45.5	76.2	0.68	Concrete	32.9	1.38	25.27	1.80
Steele[23]	38-B	2	2	2	1	0.749	2.625	3965	2328	385	107.9	0.91	3.50	8.0	4.0	0.0	6.0	40.0	76.2	0.60	Concrete	38.4	1.04	29.48	1.36
Steele[23]	36-C-2	2	2	2	1	0.749	2.625	3470	2094	366	105.1	0.93	3.50	8.0	4.0	0.0	6.0	40.8	76.2	0.61	Concrete	36.5	1.12	28.03	1.46
Steele[23]	31-B-1	2	2	2	1	0.749	2.625	4415	2592	414	111.8	0.93	3.50	8.0	4.0	0.0	6.0	40.0	76.2	0.60	Concrete	41.3	0.97	31.70	1.26
Steele[23]	34-B	2	2	2	1	0.749	2.625	3520	1878	375	97.3	0.94	3.50	8.0	4.0	0.0	6.0	35.0	76.2	0.52	Concrete	37.4	0.94	28.72	1.22
Steele[23]	34-A	2	2	2	1	0.749	2.625	3540	1676	379	90.0	0.95	3.50	8.0	4.0	0.0	6.0	38.4	76.2	0.57	Concrete	37.8	1.02	29.02	1.32
Steele[23]	37-B	2	2	2	1	0.749	2.625	3710	2466	388	114.6	0.95	3.50	8.0	4.0	0.0	6.0	42.5	76.2	0.63	Concrete	38.7	1.01	29.71	1.43
Steele[23]	38-A	2	2	2	1	0.749	2.625	2965	1827	354	101.1	0.97	3.50	8.0	4.0	0.0	6.0	35.0	76.2	0.52	Concrete	35.3	0.99	27.11	1.29
Baldwin[17]	L7B4A4	2	2	0	1	0.875	3.50	5140	2070	NR	91.5	0.75	4.00	13.0	4.0	0.0	6.0	55.6	59.0	0.78	Concrete	52.3	1.06	38.90	1.43
Baldwin[17]	L7B4B4	2	2	0	1	0.875	3.50	6110	2320	NR	93.2	0.75	4.00	13.0	4.0	0.0	6.0	50.0	59.0	0.70	Concrete	57.1	0.88	42.41	1.18
Baldwin[17]	L7B4C4	2	2	0	1	0.875	3.50	4360	2300	NR	103.7	0.75	4.00	13.0	4.0	0.0	6.0	49.6	59.0	0.70	Concrete	48.2	1.03	35.82	1.38
Baldwin[17]	L7B4D4	2	2	0	1	0.875	3.50	4360	2300	NR	103.7	0.75	4.00	13.0	4.0	0.0	6.0	53.4	59.0	0.75	Concrete	48.2	1.11	35.82	1.49
Baldwin[17]	L7B4E4	2	2	0	1	0.875	3.50	4360	2300	NR	103.7	0.75	4.00	13.0	4.0	0.0	6.0	50.4	59.0	0.71	Concrete	48.2	1.05	35.82	1.41
Baldwin[17]	L7B4F4	2	2	0	1	0.875	3.50	4190	2750	NR	118.4	0.85	4.00	13.0	4.0	0.0	6.0	55.6	59.0	0.78	Concrete	53.6	1.04	39.80	1.40
Baldwin[17]	L7B4G4	2	2	0	1	0.875	3.50	4190	2750	NR	118.4	0.85	4.00	13.0	4.0	0.0	6.0	55.6	59.0	0.78	Concrete	53.6	1.04	39.80	1.40
Chinn[24]	7BI 1-4	2	2	0	1	0.875	3.50	4000	4420	NR	93	0.75	4.00	8.0	4.0	0.0	6.0	64.0	65.1	0.82	Concrete	46.2	1.39	34.31	1.87
Dallam[20]	2(L7B4a)	2	2	0	1	0.875	3.50	5140	NR	NR	NR	0.75	4.00	13.0	4.0	0.0	6.0	55.8	59.0	0.79	Concrete	52.3	1.07	38.90	1.43
Dallam[20]	3(L7B4b)	2	2	0	1	0.875	3.50	6110	NR	NR	NR	0.75	4.00	13.0	4.0	0.0	6.0	50.0	59.0	0.70	Concrete	57.1	0.88	42.41	1.18
Baldwin[17]	L6B4A4	2	2	0	1	0.750	3.50	5050	2070	NR	92.0	0.75	4.67	13.0	4.0	0.0	6.0	38.6	59.0	0.74	Weld	41.2	0.94	38.55	1.00
Baldwin[17]	L6B4B4	2	2	0	1	0.750	3.50	4760	2480	NR	105.9	0.85	4.67	13.0	4.0	0.0	6.0	32.6	59.0	0.63	Weld	45.3	0.72	42.42	0.77
Baldwin[17]	L6B4C4	2	2	0	1	0.750	3.50	5140	2070	NR	91.5	0.75	4.67	13.0	4.0	0.0	6.0	35.0	59.0	0.67	Weld	41.5	0.84	38.90	0.90
Baldwin[17]	L6B4D4	2	2	0	1	0.750	3.50	5260	2150	NR	93.1	0.75	4.67	13.0	4.0	0.0	6.0	45.0	59.0	0.86	Concrete	42.0	1.07	39.35	1.14
Baldwin[17]	L6B4E4	2	2	0	1	0.750	3.50	5260	2150	NR	93.1	0.75	4.67	13.0	4.0	0.0	6.0	47.2	59.0	0.91	Concrete	42.0	1.12	39.35	1.20
Buttry[18]	L6B4H4	2	2	0	1	0.750	3.50	3740	1790	334	92.3	0.81	4.67	13.0	4.0	0.0	6.0	34.8	59.0	0.67	Concrete	38.5	0.90	36.03	0.97
Buttry[18]	L6H4A4	2	2	0	1	0.750	3.50	3920	1590	343	84.0	0.82	4.67	13.0	4.0	0.0	6.0	31.2	59.0	0.60	Concrete	39.5	0.79	37.03	0.84
Buttry[18]	L6H4B4	2	2	0	1	0.750	3.50	4190	1880	378	91.9	0.87	4.67	13.0	4.0	0.0	6.0	35.0	59.0	0.67	Concrete	43.6	0.80	40.81	0.86
Chinn[24]	6BI 1-4	2	2	0	1	0.750	3.50	4000	5090	NR	93	0.75	4.67	8.0	4.0	0.0	6.0	51.5	65.1	0.90	Stud	36.6	1.41	34.31	1.50
Dallam[20]	6(L6A4a)	2	2	0	1	0.750	3.50	3900	NR	NR	NR	0.75	4.67	22.5	4.0	0.0	6.0	31.8	72.1	0.50	Weld	36.2	0.88	33.88	0.94

Dallam[20]	7(L6B4a)	2	2	0	1	0.750	3.50	5050	NR	NR	NR	0.75	4.67	13.0	4.0	0.0	6.0	38.8	72.1	0.61	Weld	41.2	0.94	38.55	1.01
Dallam[20]	8(L6B4b)	2	2	0	1	0.750	3.50	4760	NR	NR	NR	0.75	4.67	13.0	4.0	0.0	6.0	33.0	72.1	0.52	Weld	40.0	0.83	37.43	0.88
Dallam[20]	9(L6B4c)	2	2	0	1	0.750	3.50	5140	NR	NR	NR	0.75	4.67	13.0	4.0	0.0	6.0	37.8	72.1	0.59	Weld	41.5	0.91	38.90	0.97
Dallam[20]	10(L6B4d)	2	2	0	1	0.750	3.50	5260	NR	NR	NR	0.75	4.67	13.0	4.0	0.0	6.0	45.0	72.1	0.71	Concrete	42.0	1.07	39.35	1.14
Dallam[20]	11(L6B4e)	2	2	0	1	0.750	3.50	5260	NR	NR	NR	0.75	4.67	13.0	4.0	0.0	6.0	47.2	72.1	0.74	Concrete	42.0	1.12	39.35	1.20
Dhir[22] and Chinn[24]	6BI 2-4	2	2	0	1	0.750	3.50	4120	2213	NR	93	0.75	4.67	8.0	4.0	0.0	6.0	45.0	67.9	0.75	Stud	37.2	1.21	34.82	1.29
Buttry[18]	L4B4A3	2	2	0	1	0.500	2.69	3070	1780	302	98.2	0.81	5.38	13.0	4.0	0.0	6.0	27.6	67.8	1.04	Concrete	16.6	1.66	23.79	1.16
Dhir[22] and Chinn[24]	4BI 2-3	2	2	0	1	0.500	2.69	5180	2418	NR	93	0.75	5.38	8.0	4.0	0.0	6.0	24.5	71.2	0.88	Stud	19.9	1.23	28.50	0.86
Dallam[20]	13(L5B4a)	2	2	0	1	0.625	3.69	5520	NR	NR	NR	0.75	5.90	13.0	4.0	0.0	6.0	36.0	64.2	0.91	Stud	33.6	1.07	42.97	0.84
Dallam[20]	14(L5B4b)	2	2	0	1	0.625	3.69	5520	NR	NR	NR	0.75	5.90	13.0	4.0	0.0	6.0	37.2	64.2	0.94	Stud	33.6	1.11	42.97	0.87
Dallam[20]	15(L5B4c)	2	2	0	1	0.625	3.69	4940	NR	NR	NR	0.75	5.90	13.0	4.0	0.0	6.0	32.4	64.2	0.82	Concrete-PD	31.8	1.02	40.65	0.80
Dallam[20]	16(L5B4d)	2	2	0	1	0.625	3.69	4720	NR	NR	NR	0.75	5.90	13.0	4.0	0.0	6.0	33.0	64.2	0.84	Concrete-PD	31.1	1.06	39.74	0.83
Baldwin[17]	L5B4C4	2	2	0	1	0.625	3.69	4940	2180	NR	96.0	0.75	5.90	13.0	4.0	0.0	6.0	32.4	64.2	0.82	Concrete	31.8	1.02	40.66	0.80
Baldwin[17]	L5B4D4	2	2	0	1	0.625	3.69	4720	2160	NR	96.8	0.75	5.90	13.0	4.0	0.0	6.0	33.0	64.2	0.84	Concrete	31.1	1.06	39.74	0.83
Buttry[18]	L5B4G4	2	2	0	1	0.625	3.69	3530	1810	324	94.8	0.81	5.90	13.0	4.0	0.0	6.0	26.4	64.2	0.67	Concrete	29.2	0.90	37.32	0.71
Baldwin[17]	L5B4A4	2	2	0	1	0.625	3.69	5520	NR	NR	NR	0.75	5.90	13.0	4.0	0.0	6.0	30.0	64.2	0.76	Stud	33.6	0.89	42.98	0.70
Baldwin[17]	L5B4B4	2	2	0	1	0.625	3.69	5520	NR	NR	NR	0.75	5.90	13.0	4.0	0.0	6.0	37.4	64.2	0.95	Stud	33.6	1.11	42.98	0.87
Dallam[20]	18(L4B4a)	2	2	0	1	0.500	3.69	5520	NR	NR	NR	0.75	7.37	13.0	4.0	0.0	6.0	17.2	78.3	0.56	Stud	24.1	0.72	42.97	0.40
Dallam[20]	19(L4B4b)	2	2	0	1	0.500	3.69	5050	NR	NR	NR	0.75	7.37	13.0	4.0	0.0	6.0	21.6	78.3	0.70	Stud	23.0	0.94	41.10	0.53
Dallam[20]	20(L4B4c)	2	2	0	1	0.500	3.69	4940	NR	NR	NR	0.75	7.37	13.0	4.0	0.0	6.0	23.8	78.3	0.77	Stud	22.8	1.05	40.65	0.59
Baldwin[17]	L4B4A4	2	2	0	1	0.500	3.69	5520	NR	NR	NR	0.75	7.38	13.0	4.0	0.0	6.0	17.2	78.3	0.56	Stud	24.1	0.72	42.98	0.40
Baldwin[17]	L4B4B4	2	2	0	1	0.500	3.69	5050	2030	NR	90.9	0.75	7.38	13.0	4.0	0.0	6.0	21.4	78.3	0.70	Stud	23.0	0.93	41.11	0.52
Baldwin[17]	L4B4C4	2	2	0	1	0.500	3.69	4940	2180	NR	96.0	0.75	7.38	13.0	4.0	0.0	6.0	23.2	78.3	0.75	Stud	22.8	1.02	40.66	0.57
Baldwin[17]	L4B4D4	2	2	0	1	0.500	3.69	7740	2330	NR	86.4	0.75	7.38	13.0	4.0	0.0	6.0	26.2	78.3	0.85	Stud	28.5	0.92	50.89	0.51
Baldwin[17]	L4B4E4	2	2	0	1	0.500	3.69	8080	2640	NR	92.5	0.75	7.38	13.0	4.0	0.0	6.0	24.8	78.3	0.81	Stud	29.1	0.85	52.00	0.48
Baldwin[17]	L4B4F4	2	2	0	1	0.500	3.69	8080	2640	NR	92.5	0.75	7.38	13.0	4.0	0.0	6.0	24.8	78.3	0.81	Stud	29.1	0.85	52.00	0.48
Buttry[18]	L4B4G4	2	2	0	1	0.500	3.69	3030	1690	300	95.3	0.81	7.38	13.0	4.0	0.0	6.0	21.4	78.3	0.70	Stud	19.3	1.11	34.57	0.62
Normal Weight Concrete - Single Y Row																									
Zhao[10]	1	1	1	0	0	0.866	1.97	3133	3190	375	145	1.00	2.27	NR	0.0	0.0	NR	13.3	61.9	0.36	Pryout	20.1	0.66	6.18	2.15
Zhao[10]	2	1	1	0	0	0.866	1.97	3133	3190	375	145	1.00	2.27	NR	0.0	0.0	NR	17.7	61.9	0.49	Pryout	20.1	0.88	6.18	2.86
Zhao[10]	3	1	1	0	0	0.866	1.97	3133	3190	375	145	1.00	2.27	NR	0.0	0.0	NR	17.8	61.9	0.49	Pryout	20.1	0.89	6.18	2.88
Buttry[18]	N6B4A2	2	2	0	1	0.750	1.50	5640	4100	502	139.9	1.00	2.00	13.0	4.0	0.0	6.0	38.6	62.1	0.70	Pull-out	38.0	1.02	10.42	3.70
Hawkins[26]	J27.36	2	2	0	1	0.875	1.75	3620	3430	399	145	1.00	2.00	14.0	3.6	0.0	4.0	41.1	61.90	0.55	Pull-out	41.4	0.99	9.42	4.37
Hawkins[26]	M26.42	2	2	0	1	0.750	1.75	4250	3716	472	145	1.00	2.33	14.0	3.6	0.0	4.0	41.4	78.20	0.60	Pull-out	35.6	1.16	10.21	4.06
Hawkins[26]	J26.49	2	2	0	1	0.750	1.75	4850	3970	467	145	1.00	2.33	14.0	3.6	0.0	4.0	42.6	66.80	0.72	Pull-out	38.0	1.12	10.90	3.91
Viest[14]	10A2	2	2	0	1	1.250	3.09	3190	3219	378	145	1.00	2.47	18.0	4.1	0.0	7.0	100.0	63.80	0.64	Concrete	88.2	1.13	35.45	2.82
Viest[14]	10B2	2	2	0	1	1.250	3.19	3500	3372	396	145	1.00	2.55	18.0	4.1	0.0	7.0	95.0	63.60	0.61	Concrete	93.9	1.01	38.57	2.46
Hawkins[26]	M37.51	2	2	0	1	0.875	2.5	5110	4075	479	145	1.00	2.86	14.0	3.6	0.0	4.0	52.4	76.60	0.57	Pull-out	58.8	0.89	33.53	1.56
Hawkins[26]	J37.44	2	2	0	1	0.875	2.5	4430	3794	460	145	1.00	2.86	14.0	3.6	0.0	4.0	47.6	61.50	0.64	Pull-out	54.8	0.87	31.22	1.53
Zhao[10]	4	1	1	0	0	0.866	2.56	3133	3190	375	145	1.00	2.96	NR	0.0	0.0	NR	18.9	61.9	0.52	Pryout	22.9	0.82	18.33	1.03
Zhao[10]	5	1	1	0	0	0.866	2.56	3133	3190	375	145	1.00	2.96	NR	0.0	0.0	NR	21.2	61.9	0.58	Pryout	22.9	0.92	18.33	1.16
Zhao[10]	6	1	1	0	0	0.866	2.56	3133	3190	375	145	1.00	2.96	NR	0.0	0.0	NR	19.5	61.9	0.53	Pryout	22.9	0.85	18.33	1.06
Hawkins[9]	6S	1	1	0	1	1.0	3	3100	3174	373	145	1.00	3.00	9	0	0	9	19.5	134	0.25	Concrete-Radial	30.7	0.64	23.14	0.84
Hawkins[9]	1S	1	1	0	1	1.0	3	3080	3163	372	145	1.00	3.00	9	0	0	9	23.7	134	0.30	Pullout	30.6	0.78	23.07	1.03
Hawkins[9]	3S	1	1	0	1	1.0	3	2900	3070	361	145	1.00	3.00	9	0	0	9	22.1	134	0.28	Pullout	29.6	0.74	22.39	0.99
Hawkins[9]	7S	1	1	0	1	1.0	3	4930	4002	470	145	1.00	3.00	9	0	0	9	27.2	134	0.34	Pullout	38.7	0.70	29.19	0.93
Viest[14]	8B2	2	2	0	1	1.000	3.22	4230	3707	436	145	1.00	3.22	18.0	3.8	0.0	7.0	90.0	73.60	0.78	Concrete	74.2	1.21	41.89	2.15
Viest[14]	8A2	2	2	0	1	1.000	3.23	3760	3495	411	145	1.00	3.23	18.0	3.8	0.0	7.0	84.0	73.60	0.73	Concrete	70.1	1.20	39.64	2.12
Buttry[18]	N6B4A3	2	2	0	1	0.750	2.50	3290	3140	383	140.2	1.00	3.33	13.0	4.0	0.0	6.0	44.0	62.1	0.80	Concrete	37.4	1.18	27.81	1.58
Buttry[18]	N6B4B3	2	2	0	1	0.750	2.50	6230	4140	527	136.2	1.00	3.33	13.0	4.0	0.0	6.0	48.4	62.1	0.88	Concrete	51.5	0.94	38.27	1.26
Hawkins[26]	M36.42	2	2	0	1	0.750	2.5	4230	3707	416	145	1.00	3.33	14.0	3.6	0.0	4.0	49.2	61.80	0.90	Concrete	42.5	1.16	30.51	1.61
Hawkins[26]	J36.58	2	2	0	1	0.750	2.5	5790	4337	510	145	1.00	3.33	14.0	3.6	0.0	4.0	49.9	75.70	0.75	Concrete	49.7	1.01	35.69	1.40
Dhir[22] and Chinn[24]	6BS 4-3	2	2	0	1	0.750	2.50	5040	3215	NR	145	1.00	3.33	8.0	4.0	0.0	6.0	55.0	72.1	0.86	Stud	46.4	1.19	34.42	1.60
Buttry[18]	N4B4A2	2	2	0	1	0.500	1.69	3900	3600	417	145.1	1.00	3.38	13.0	4.0	0.0	6.0	22.4	75.5	0.76	Stud	18.2	1.23	9.80	2.29
Buttry[18]	N4B4B2	2	2	0	1	0.500	1.69	5200	4140	482	144.7	1.00	3.38	13.0	4.0	0.0	6.0	25.0	75.5	0.84	Stud	21.1	1.19	11.32	2.21
Buttry[18]	N5H4B2.5	2	2	0	1	0.625	2.19	4560	3830	445	143.5	1.00	3.50	13.0	4.0	0.0	6.0	29.2	64.2	0.74	Pull-out	31.4	0.93	14.07	2.08
Hawkins & Mitchell[38]	1M	2	2	0	1	0.750	2.63	3310	3279	386	145	1.00	3.50	16.0	3.0	0.0	4.0	57.0	74.5	0.87	Stud	38.5	1.48	27.03	2.11
Ollgaard et al.[5]	2B(1)	2	2	0	1	0.750	2.63	4780	3180	470	140.5	1.00	3.50	14.0	4.0	0.0	6.0	52.2	70.9	0.83	Stud	46.3	1.13	35.47	1.47
Ollgaard et al.[5]	2B(2)	2	2	0	1	0.750	2.63	4780	3180	470	140.5	1.00	3.50	14.0	4.0	0.0	6.0	51.0	70.9	0.81	Stud	46.3	1.10	35.47	1.44
Ollgaard et al.[5]	2B(3)	2	2	0	1	0.750	2.63	4780	3180	470	140.5	1.00	3.50	14.0	4.0	0.0	6.0	50.0	70.9	0.80	Stud	46.3	1.08	35.47	1.41
Steele[23]	30-C	2	2	2	1	0.749	2.625	3355	1756	387	94.5	1.00	3.50	8.0	4.0	0.0	6.0	34.5	76.2	0.51	Concrete	38.6	0.89	29.63	1.16
Steele[23]	38-C	2	2	2	1	0.749	2.625	3685	1589	425	85.7	1.00	3.50	8.0	4.0	0.0	6.0	43.8	76.2	0.65	Concrete	40.5	1.08	31.14	1.41

(1)	(2)	(3)	(4)	(5)	(6)	(7)	(8)	(9)	(10)	(11)	(12)	(13)	(14)	(15)	(16)	(17)	(18)	(19)	(20)	(21)	(22)	(23)	(24)	(25)	(26)
Investigators	**Test number**	**No. of studs, n**	**Front row (FR)**	**Back row (BR)**	**Side row (SR)**	**Stud dia., d (in.)**	**Embed depth, h_{ef} (in.)**	**Concrete strength, f'_c (psi)**	**Concrete modulus, E_c (ksi)**	**Concrete splitting strength, f_{sp} (psi)**	**Concrete density, w_c (lb/ft³)**	**LW factor, λ**	**h_{ef}/d**	**Test geometry**				**1 side V test (kips)**	**Stud strength, F_u (ksi)**	**Steel ratio, Test / Pred**	**Report failure mode**	**$V_{poc} = V_{po} * \psi_y$ (kips)**	**Test / Pred**	**ACI V_{sp} (kips)**	**Test / Pred**
														d_{e3} (in.)	x (in.)	y (in.)	h (in.)								
Steele[23]	CoS&G	2	2	2	1	0.749	2.625	2875	3056	354	144.0	0.99	3.50	8.0	4.0	0.0	6.0	51.6	76.2	0.77	Concrete	35.3	1.46	27.11	1.90
Baldwin[17]	N7B4A4	2	2	0	1	0.875	3.50	5860	4880	NR	155.1	1.00	4.00	13.0	4.0	0.0	6.0	60.0	59.0	0.85	Concrete	74.5	0.81	55.38	1.08
Dallam[20]	1(N7B4a)	2	2	0	1	0.875	3.50	5730	4315	507	145	1.00	4.00	13.0	4.0	0.0	6.0	64.4	59.0	0.91	Concrete	73.7	0.87	54.76	1.18
Hawkins[9]	13S	1	1	0	1	0.75	3	3080	3163	372	145	1.00	4.00	9	0	0	9	20.22	134	0.46	Concrete-Radial	19.8	1.02	23.07	0.88
Hawkins[9]	11S	1	1	0	1	0.75	3	3040	3143	369	145	1.00	4.00	9	0	0	9	23.1	134	0.52	Pullout	19.7	1.17	22.92	1.01
Hawkins[9]	14S	1	1	0	1	0.75	3	5040	4047	476	145	1.00	4.00	9	0	0	9	28.25	134	0.64	Pullout	25.4	1.11	29.51	0.96
Zhao[10]	7	1	1	0	0	0.866	3.54	3133	3190	375	145	1.00	4.09	NR	0.0	0.0	NR	29.8	61.9	0.82	Pryout	27.0	1.10	29.87	1.00
Zhao[10]	8	1	1	0	0	0.866	3.54	3133	3190	375	145	1.00	4.09	NR	0.0	0.0	NR	29.4	61.9	0.81	Pryout	27.0	1.09	29.87	0.98
Zhao[10]	9	1	1	0	0	0.866	3.54	3133	3190	375	145	1.00	4.09	NR	0.0	0.0	NR	31.1	61.9	0.85	Pryout	27.0	1.15	29.87	1.04
Baldwin[17]	N6B4A4	2	2	0	1	0.750	3.50	5860	4880	NR	155.1	1.00	4.67	13.0	4.0	0.0	6.0	58.8	59.0	1.13	Concrete	59.1	0.99	55.38	1.06
Buttry[18]	N6B4B4	2	2	0	1	0.750	3.50	3410	3330	390	144.0	1.00	4.67	13.0	4.0	0.0	6.0	42.2	59.0	0.81	Concrete	45.1	0.94	42.24	1.00
Buttry[18]	N6H4A4	2	2	0	1	0.750	3.50	4190	3970	452	151.2	1.00	4.67	13.0	4.0	0.0	6.0	41.6	59.0	0.80	Concrete	50.0	0.83	46.83	0.89
Buttry[18]	N6H4B4	2	2	0	1	0.750	3.50	4540	3770	428	142.2	1.00	4.67	13.0	4.0	0.0	6.0	45.0	59.0	0.86	Concrete	52.1	0.86	48.74	0.92
Dallam[20]	5(N6B4a)	2	2	0	1	0.750	3.50	5730	4315	507	145	1.00	4.67	13.0	4.0	0.0	6.0	58.8	72.1	0.92	Concrete	58.5	1.01	54.76	1.07
Hawkins[26]	J46.44	2	2	0	1	0.750	3.5	4440	3798	435	145	1.00	4.67	14.0	3.6	0.0	5.0	53.8	76.20	0.80	Concrete	51.5	1.05	46.96	1.15
Hawkins[26]	M46.26	2	2	0	1	0.750	3.5	2680	2951	305	145	1.00	4.67	14.0	3.6	0.0	5.0	38.0	72.80	0.59	Concrete	40.0	0.95	36.48	1.04
Hawkins[26]	J46.19	2	2	0	1	0.750	3.5	1980	2536	198	145	1.00	4.67	14.0	3.6	0.0	5.0	37.4	74.30	0.57	Concrete	34.4	1.09	31.36	1.19
Hawkins[26]	ML46.47	2	2	0	1	0.750	3.5	4750	3929	362	145	1.00	4.67	14.0	3.6	0.0	5.0	41.8	67.80	0.70	Concrete	53.2	0.79	48.57	0.86
Hawkins[26]	JL46.56	2	2	0	1	0.750	3.5	4510	3828	388	145	1.00	4.67	14.0	3.6	0.0	5.0	45.9	72.80	0.71	Concrete	51.9	0.89	47.32	0.97
Viest[14]	6A4	4	4	0	1	0.750	3.50	3360	3304	388	145	1.00	4.67	18.0	1.9	0.0	7.0	84.8	67.70	0.71	Concrete	89.6	0.95	46.50	1.82
Davies[25]	P41	2	2	0	1	0.375	1.75	5520	4235	498	145	1.00	4.67	4.5	1.5	0.0	2.5	14.7	76.2	0.87	Mixed	14.3	1.02	8.85	1.66
Davies[25]	P51	2	2	0	1	0.375	1.75	5280	4142	487	145	1.00	4.67	4.5	1.5	0.0	2.5	15.8	76.2	0.94	Mixed	14.0	1.13	8.65	1.83
Davies[25]	P61	2	2	0	1	0.375	1.75	4240	3712	436	145	1.00	4.67	4.5	1.5	0.0	2.5	11.8	76.2	0.70	Mixed	12.6	0.94	7.75	1.52
Davies[25]	P71	2	2	0	1	0.375	1.75	4560	3849	452	145	1.00	4.67	4.5	1.5	0.0	2.5	12.0	76.2	0.71	Mixed	13.0	0.92	8.04	1.49
Davies[25]	P81	2	2	0	1	0.375	1.75	3760	3495	411	145	1.00	4.67	4.5	1.5	0.0	2.5	11.2	76.2	0.67	Mixed	11.8	0.95	7.30	1.53
Davies[25]	P82	2	2	0	1	0.375	1.75	3760	3495	411	145	1.00	4.67	4.5	0.8	0.0	2.5	9.8	76.2	0.58	Mixed	11.8	0.83	6.49	1.51
Hawkins[26]	MR46.32	2	2	0	1	0.750	3.5	3270	3260	379	145	1.00	4.67	14.0	3.6	0.0	5.0	49.0	70.90	0.78	Punch-out	44.2	1.11	40.30	1.21
Hawkins[26]	MR46.37	2	2	0	1	0.750	3.5	3700	3467	441	145	1.00	4.67	14.0	3.6	0.0	5.0	52.9	70.90	0.84	Punch-out	47.0	1.13	42.86	1.23
Dhir[22] and Chinn[24]	6BS 5-4	2	2	0	1	0.750	3.50	4680	3039	NR	145	1.00	4.67	8.0	4.0	0.0	6.0	50.5	67.9	0.84	Stud	52.8	0.96	49.49	1.02
Hawkins[26]	M46.89	2	2	0	1	0.750	3.5	8990	5405	591	145	1.00	4.67	14.0	3.6	0.0	5.0	66.9	65.00	1.16	Stud	73.2	0.91	66.81	1.00
Viest[14]	6B4	4	4	0	1	0.750	3.58	3260	3255	383	145	1.00	4.77	18.0	1.9	0.0	7.0	90.0	69.30	0.74	Concrete	89.2	1.01	47.45	1.90
Multiple Y Row																									
Zhao[10]	1a	4	2	2	2	0.866	1.97	3365	3306	389	145	1.00	2.27	NR	3.94	3.94	NR	38.4	61.9	0.26	Pryout	47.8	0.80	17.81	2.15
Zhao[10]	2a	4	2	2	2	0.866	1.97	3365	3306	389	145	1.00	2.27	NR	3.94	3.94	NR	37.0	61.9	0.25	Pryout	47.8	0.78	17.81	2.08
Zhao[10]	3a	4	2	2	2	0.866	1.97	3365	3306	389	145	1.00	2.27	NR	3.94	3.94	NR	38.6	61.9	0.26	Pryout	47.8	0.81	17.81	2.17
Zhao[10]	1b	4	2	2	2	0.866	2.56	3365	3306	389	145	1.00	2.96	NR	3.94	3.94	NR	49.0	61.9	0.34	Pryout	54.5	0.90	43.50	1.13
Zhao[10]	2b	4	2	2	2	0.866	2.56	3365	3306	389	145	1.00	2.96	NR	3.94	3.94	NR	51.1	61.9	0.35	Pryout	54.5	0.94	43.50	1.18
Zhao[10]	3b	4	2	2	2	0.866	2.56	3365	3306	389	145	1.00	2.96	NR	3.94	3.94	NR	51.7	61.9	0.35	Pryout	54.5	0.95	43.50	1.19
An & Cederwall[39]	HSC11	4	2	2	2	0.750	2.63	12,489	4945	749	149	1.00	3.50	9.8	5.9	9.8	5.9	141.0	75.2	1.06	Mixed	156.4	0.90	133.12	1.06
An & Cederwall[39]	HSC12	4	2	2	2	0.750	2.63	11,786	4945	727	149	1.00	3.50	9.8	5.9	9.8	5.9	142.6	75.2	1.07	Mixed	151.9	0.94	129.32	1.10
An & Cederwall[39]	HSC21	4	2	2	2	0.750	2.63	11,786	4945	727	149	1.00	3.50	9.8	5.9	9.8	5.9	136.6	75.2	1.03	Mixed	151.9	0.90	129.32	1.06
An & Cederwall[39]	HSC22	4	2	2	2	0.750	2.63	13,233	4945	771	150	1.00	3.50	9.8	5.9	9.8	5.9	144.8	75.2	1.09	Mixed	160.9	0.90	137.03	1.06
An & Cederwall[39]	NSC11	4	2	2	2	0.750	2.63	4463	3930	448	147	1.00	3.50	9.8	5.9	9.8	5.9	103.4	75.2	0.78	Mixed	93.5	1.11	79.57	1.30
An & Cederwall[39]	NSC12	4	2	2	2	0.750	2.63	4463	3920	448	147	1.00	3.50	9.8	5.9	9.8	5.9	100.3	75.2	0.75	Mixed	93.5	1.07	79.57	1.26
An & Cederwall[39]	NSC21	4	2	2	2	0.750	2.63	4463	3920	448	147	1.00	3.50	9.8	5.9	9.8	5.9	108.6	75.2	0.82	Mixed	93.5	1.16	79.57	1.37
An & Cederwall[39]	NSC22	4	2	2	2	0.750	2.63	4611	3975	455	146	1.00	3.50	9.8	5.9	9.8	5.9	107.1	75.2	0.81	Mixed	95.0	1.13	80.88	1.32
Ollgaard et al.[5]	C-(1)	4	2	2	2	0.750	2.63	4670	1510	240	89.1	0.75	3.50	8.0	4.0	12.0	6.0	79.6	70.9	0.64	Concrete	79.2	1.01	52.59	1.51
Ollgaard et al.[5]	C-(2)	4	2	2	2	0.750	2.63	4670	1510	240	89.1	0.75	3.50	8.0	4.0	12.0	6.0	85.2	70.9	0.68	Concrete	79.2	1.08	52.59	1.62
Ollgaard et al.[5]	C-(3)	4	2	2	2	0.750	2.63	4670	1510	240	89.1	0.75	3.50	8.0	4.0	12.0	6.0	84.0	70.9	0.67	Concrete	79.2	1.06	52.59	1.60
Ollgaard et al.[5]	D-(1)	4	2	2	2	0.750	2.63	4720	2430	320	99.2	0.75	3.50	8.0	4.0	12.0	6.0	96.4	70.9	0.77	Concrete	79.6	1.21	52.87	1.82
Ollgaard et al.[5]	D-(2)	4	2	2	2	0.750	2.63	4720	2430	320	99.2	0.75	3.50	8.0	4.0	12.0	6.0	92.0	70.9	0.73	Concrete	79.6	1.16	52.87	1.74
Ollgaard et al.[5]	D-(3)	4	2	2	2	0.750	2.63	4720	2430	320	99.2	0.75	3.50	8.0	4.0	12.0	6.0	90.8	70.9	0.72	Concrete	79.6	1.14	52.87	1.72
Ollgaard et al.[5]	E-(1)	4	2	2	2	0.750	2.63	3600	1840	300	97.7	0.75	3.50	8.0	4.0	12.0	6.0	78.4	70.9	0.63	Concrete	69.5	1.13	46.18	1.70
Ollgaard et al.[5]	E-(2)	4	2	2	2	0.750	2.63	3600	1840	300	97.7	0.75	3.50	8.0	4.0	12.0	6.0	76.8	70.9	0.61	Concrete	69.5	1.10	46.18	1.66
Ollgaard et al.[5]	E-(3)	4	2	2	2	0.750	2.63	3600	1840	300	97.7	0.75	3.50	8.0	4.0	12.0	6.0	71.2	70.9	0.57	Concrete	69.5	1.02	46.18	1.54
Ollgaard et al.[5]	D(1)	4	2	2	2	0.750	2.63	4920	2530	360	113.4	0.77	3.50	8.0	4.0	12.0	6.0	86.4	70.9	0.69	Concrete	83.0	1.04	55.13	1.57

Ollgaard et al.[5]	D(2)	4	2	2	2	0.750	2.63	4920	2530	360	113.4	0.77	3.50	8.0	4.0	12.0	6.0	93.2	70.9	0.74	Concrete	83.0	1.12	55.13	1.69
Ollgaard et al.[5]	D(3)	4	2	2	2	0.750	2.63	4920	2530	360	113.4	0.77	3.50	8.0	4.0	12.0	6.0	97.6	70.9	0.78	Concrete	83.0	1.18	55.13	1.77
Ollgaard et al.[5]	SE(1)	4	2	2	2	0.625	2.19	4000	2060	330	112.3	0.78	3.50	8.0	4.0	12.0	6.0	62.8	70.9	0.72	Concrete	63.4	0.99	20.52	3.06
Ollgaard et al.[5]	SE(2)	4	2	2	2	0.625	2.19	4000	2060	330	112.3	0.78	3.50	8.0	4.0	12.0	6.0	62.8	70.9	0.72	Concrete	63.4	0.99	20.52	3.06
Ollgaard et al.[5]	SE(3)	4	2	2	2	0.625	2.19	4000	2060	330	112.3	0.78	3.50	8.0	4.0	12.0	6.0	68.0	70.9	0.78	Concrete	63.4	1.07	20.52	3.31
Ollgaard et al.[5]	C(1)	4	2	2	2	0.750	2.63	4280	2060	350	108.2	0.80	3.50	8.0	4.0	12.0	6.0	86.4	70.9	0.69	Concrete	80.7	1.07	53.60	1.61
Ollgaard et al.[5]	C(2)	4	2	2	2	0.750	2.63	4280	2060	350	108.2	0.80	3.50	8.0	4.0	12.0	6.0	86.0	70.9	0.69	Concrete	80.7	1.07	53.60	1.60
Ollgaard et al.[5]	C(3)	4	2	2	2	0.750	2.63	4280	2060	350	108.2	0.80	3.50	8.0	4.0	12.0	6.0	88.8	70.9	0.71	Concrete	80.7	1.10	53.60	1.66
Ollgaard et al.[5]	LE(1)	4	2	2	2	0.750	2.63	3220	1880	320	111.4	0.84	3.50	8.0	4.0	12.0	6.0	74.8	70.9	0.60	Concrete	73.8	1.01	49.01	1.53
Ollgaard et al.[5]	LE(2)	4	2	2	2	0.750	2.63	3220	1880	320	111.4	0.84	3.50	8.0	4.0	12.0	6.0	78.0	70.9	0.62	Concrete	73.8	1.06	49.01	1.59
Ollgaard et al.[5]	LE(3)	4	2	2	2	0.750	2.63	3220	1880	320	111.4	0.84	3.50	8.0	4.0	12.0	6.0	78.8	70.9	0.63	Concrete	73.8	1.07	49.01	1.61
Ollgaard et al.[5]	E(1)	4	2	2	2	0.750	2.63	4300	2190	370	111.1	0.84	3.50	8.0	4.0	12.0	6.0	92.4	70.9	0.74	Concrete	85.3	1.08	56.67	1.63
Ollgaard et al.[5]	E(2)	4	2	2	2	0.750	2.63	4300	2190	370	111.1	0.84	3.50	8.0	4.0	12.0	6.0	90.0	70.9	0.72	Concrete	85.3	1.05	56.67	1.59
Ollgaard et al.[5]	E(3)	4	2	2	2	0.750	2.63	4300	2190	370	111.1	0.84	3.50	8.0	4.0	12.0	6.0	86.4	70.9	0.69	Concrete	85.3	1.01	56.67	1.52
Ollgaard et al.[5]	LB(1)	4	2	2	2	0.750	2.63	2670	2190	320	138.6	0.92	3.50	8.0	4.0	12.0	6.0	73.2	70.9	0.58	Concrete	73.8	0.99	49.01	1.49
Ollgaard et al.[5]	LB(2)	4	2	2	2	0.750	2.63	2670	2190	320	138.6	0.92	3.50	8.0	4.0	12.0	6.0	72.4	70.9	0.58	Concrete	73.8	0.98	49.01	1.48
Ollgaard et al.[5]	LB(3)	4	2	2	2	0.750	2.63	2670	2190	320	138.6	0.92	3.50	8.0	4.0	12.0	6.0	69.2	70.9	0.55	Concrete	73.8	0.94	49.01	1.41
Ollgaard et al.[5]	A(1)	4	2	2	2	0.750	2.63	5080	3740	510	148.1	1.00	3.50	8.0	4.0	12.0	6.0	117.2	70.9	0.94	Concrete	110.1	1.06	73.14	1.60
Ollgaard et al.[5]	A(2)	4	2	2	2	0.750	2.63	5080	3740	510	148.1	1.00	3.50	8.0	4.0	12.0	6.0	130.0	70.9	1.04	Concrete	110.1	1.18	73.14	1.78
Ollgaard et al.[5]	A(3)	4	2	2	2	0.750	2.63	5080	3740	510	148.1	1.00	3.50	8.0	4.0	12.0	6.0	122.4	70.9	0.98	Concrete	110.1	1.11	73.14	1.67
Ollgaard et al.[5]	B(1)	4	2	2	2	0.750	2.63	4780	3180	470	140.5	1.00	3.50	8.0	4.0	12.0	6.0	109.6	70.9	0.87	Concrete	106.8	1.03	70.94	1.54
Ollgaard et al.[5]	B(2)	4	2	2	2	0.750	2.63	4780	3180	470	140.5	1.00	3.50	8.0	4.0	12.0	6.0	101.6	70.9	0.81	Concrete	106.8	0.95	70.94	1.43
Ollgaard et al.[5]	B(3)	4	2	2	2	0.750	2.63	4780	3180	470	140.5	1.00	3.50	8.0	4.0	12.0	6.0	101.6	70.9	0.81	Concrete	106.8	0.95	70.94	1.43
Ollgaard et al.[5]	LA(1)	4	2	2	2	0.750	2.63	3640	3510	430	147.6	1.00	3.50	8.0	4.0	12.0	6.0	98.0	70.9	0.78	Concrete	93.2	1.05	61.91	1.58
Ollgaard et al.[5]	LA(2)	4	2	2	2	0.750	2.63	3640	3510	430	147.6	1.00	3.50	8.0	4.0	12.0	6.0	106.0	70.9	0.85	Concrete	93.2	1.14	61.91	1.71
Ollgaard et al.[5]	LA(3)	4	2	2	2	0.750	2.63	3640	3510	430	147.6	1.00	3.50	8.0	4.0	12.0	6.0	98.8	70.9	0.79	Concrete	93.2	1.06	61.91	1.60
Ollgaard et al.[5]	SA(1)	4	2	2	2	0.625	2.19	4010	3580	430	147.4	1.00	3.50	8.0	4.0	12.0	6.0	78.0	70.9	0.90	Concrete	81.5	0.96	26.38	2.96
Ollgaard et al.[5]	SA(2)	4	2	2	2	0.625	2.19	4010	3580	430	147.4	1.00	3.50	8.0	4.0	12.0	6.0	83.2	70.9	0.96	Concrete	81.5	1.02	26.38	3.15
Ollgaard et al.[5]	SA(3)	4	2	2	2	0.625	2.19	4010	3580	430	147.4	1.00	3.50	8.0	4.0	12.0	6.0	79.6	70.9	0.91	Concrete	81.5	0.98	26.38	3.02
Ollgaard et al.[5]	SB(1)	4	2	2	2	0.625	2.19	4030	3170	460	142.6	1.00	3.50	8.0	4.0	12.0	6.0	72.8	70.9	0.84	Concrete	81.7	0.89	26.45	2.75
Ollgaard et al.[5]	SB(2)	4	2	2	2	0.625	2.19	4030	3170	460	142.6	1.00	3.50	8.0	4.0	12.0	6.0	67.6	70.9	0.78	Concrete	81.7	0.83	26.45	2.56
Ollgaard et al.[5]	SB(3)	4	2	2	2	0.625	2.19	4030	3170	460	142.6	1.00	3.50	8.0	4.0	12.0	6.0	75.2	70.9	0.86	Concrete	81.7	0.92	26.45	2.84
Anderson & Meinheit*	PO4F-12A	4	2	2	2	0.5	1.81	6230	4499	529	145	1.00	3.62	39.0	3.0	6.0	15.0	58.2	75.5	0.98	Mixed	58.5	1.00	23.87	2.44
Anderson & Meinheit*	PO4F-12B	4	2	2	2	0.5	1.81	6230	4499	529	145	1.00	3.62	39.0	3.0	6.0	15.0	56.8	75.5	0.96	Pryout	58.5	0.97	23.87	2.38
Anderson & Meinheit*	PO4F-6A	4	2	2	2	0.5	1.81	5860	4363	513	145	1.00	3.62	16.5	3.0	3.0	15.0	43.8	75.5	0.74	Pryout	40.1	1.09	17.97	2.44
Anderson & Meinheit*	PO4F-6C	4	2	2	2	0.5	1.81	5920	4386	516	145	1.00	3.62	16.5	3.0	3.0	15.0	32.6	75.5	0.55	Pryout	40.3	0.81	18.06	1.80
Anderson & Meinheit*	PO4F-9A	4	2	2	2	0.5	1.81	5870	4367	513	145	1.00	3.62	15.8	3.0	4.5	15.0	41.5	75.5	0.70	Pryout	49.1	0.84	21.19	1.96
Anderson & Meinheit*	PO4F-9B	4	2	2	2	0.5	1.81	5860	4363	513	145	1.00	3.62	15.8	3.0	4.5	15.0	45.5	75.5	0.77	Pryout	49.1	0.93	21.17	2.15
Anderson & Meinheit*	PO6F-6A	6	2	2	3	0.5	1.81	6230	4499	529	145	1.00	3.62	39.0	3.0	3.0	15.0	60.1	75.5	0.68	Pryout	62.0	0.97	25.12	2.39
Anderson & Meinheit*	PO6F-6B	6	2	2	3	0.5	1.81	6230	4499	529	145	1.00	3.62	39.0	3.0	3.0	15.0	63.3	75.5	0.71	Pryout	62.0	1.02	25.12	2.52
Zhao[10]	1c	4	2	2	2	0.866	3.54	3365	3306	389	145	1.00	4.09	NR	3.94	3.94	NR	61.0	61.9	0.42	Pryout	64.1	0.95	58.15	1.05
Zhao[10]	2c	4	2	2	2	0.866	3.54	3365	3306	389	145	1.00	4.09	NR	3.94	3.94	NR	66.5	61.9	0.46	Pryout	64.1	1.04	58.15	1.14
Zhao[10]	3c	4	2	2	2	0.866	3.54	3365	3306	389	145	1.00	4.09	NR	3.94	3.94	NR	57.8	61.9	0.40	Pryout	64.1	0.90	58.15	0.99
Jayas & Hosain[40]	JS-5	8	2	2	4	0.625	2.69	4380	3975	443	145	1.00	4.30	8.0	3.0	4.0	4.0	152.0	65.0	0.95	Concrete	109.1	1.39	79.65	1.91
Davies[25]	P42	2	1	1	2	0.375	1.75	5520	4235	498	145	1.00	4.67	3.8	0.0	1.5	2.5	12.2	76.2	0.72	Mixed	11.7	1.04	8.85	1.38
Davies[25]	P43	3	1	1	3	0.375	1.75	5520	4235	498	145	1.00	4.67	3.0	0.0	1.5	2.5	15.0	76.2	0.59	Mixed	17.6	0.85	10.81	1.39
Davies[25]	P44	4	1	1	4	0.375	1.75	5520	4235	498	145	1.00	4.67	2.3	0.0	1.5	2.5	20.0	76.2	0.59	Mixed	23.4	0.85	12.78	1.57
Davies[25]	P52	2	1	1	2	0.375	1.75	5280	4142	487	145	1.00	4.67	3.8	0.0	1.5	2.5	12.6	76.2	0.75	Mixed	11.5	1.10	8.65	1.46
Davies[25]	P53	4	2	2	2	0.375	1.75	5280	4142	487	145	1.00	4.67	3.8	1.5	1.5	2.5	21.6	76.2	0.64	Mixed	22.9	0.94	11.12	1.94
Davies[25]	P54	4	1	1	4	0.375	1.75	5280	4142	487	145	1.00	4.67	2.3	0.0	1.5	2.5	21.6	76.2	0.64	Mixed	22.9	0.94	12.50	1.73
Davies[25]	P62	2	1	1	2	0.375	1.75	4240	3712	436	145	1.00	4.67	2.6	0.0	3.8	2.5	11.7	76.2	0.70	Mixed	16.2	0.72	10.34	1.13
Davies[25]	P63	2	1	1	2	0.375	1.75	4240	3712	436	145	1.00	4.67	3.8	0.0	1.5	2.5	9.6	76.2	0.57	Mixed	10.3	0.94	7.75	1.24
Davies[25]	P64	2	1	1	2	0.375	1.75	4240	3712	436	145	1.00	4.67	4.1	0.0	0.8	2.5	8.2	76.2	0.49	Mixed	7.3	1.13	6.89	1.19
Davies[25]	P72	3	1	1	3	0.375	1.75	4560	3849	452	145	1.00	4.67	2.3	0.0	2.3	2.5	15.4	76.2	0.61	Mixed	19.6	0.79	11.61	1.33
Davies[25]	P73	3	1	1	3	0.375	1.75	4560	3849	452	145	1.00	4.67	3.0	0.0	1.5	2.5	13.2	76.2	0.52	Mixed	16.0	0.83	9.83	1.34
Davies[25]	P74	3	1	1	3	0.375	1.75	4560	3849	452	145	1.00	4.67	3.8	0.0	0.8	2.5	10.8	76.2	0.43	Mixed	11.3	0.96	8.04	1.34
Davies[25]	P83	4	2	2	2	0.375	1.75	3760	3495	411	145	1.00	4.67	4.1	1.5	0.8	2.5	15.2	76.2	0.45	Mixed	13.7	1.11	8.34	1.82
Hawkins[26]	MT46.51	4	2	2	2	0.750	3.5	5140	4087	480	145	1.00	4.67	10.0	3.6	12.0	5.0	92.4	78.1	0.67	Concrete	127.9	0.72	101.04	0.91

*Present study

APPENDIX C – DESIGN EXAMPLES

Illustrative Problem 1 shows that four studs spaced apart a sufficient distance can cause the steel failure mode to control. The base equation is modified by the ψ_y factor, which is greater than 1.0 in this case. The factor is greater than 1.0 because the base equation is not fully accounting for the benefit of spreading the studs out in the *y*-direction. Hence, the modification is 1.41. This factor will have a cap on it, dictated by limiting the *y*/*d* ratio to 20.

Illustrative Problem 2 shows that adding two studs between the previous four-stud anchorage group provides a "disruption" to the connection and stress state in the concrete below the plate. If the spacing was less than the 4 in. in the problem, the ψ_y factor would actually be less than 1.0, indicating the closer spacing affects the capacity to a greater extent.

Problem 1

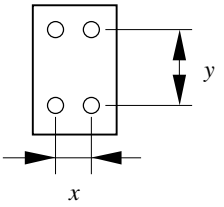

Given:

4 – ½ in. diameter × 2⅛ nominal headed studs
F_{ut} = 65 ksi (per AWS)
x = 4 in., y = 8 in., ½ in. thick plate
f'_c = 5000 psi

Problem:

Find the connection capacity away from all edges.

Solution:

Determine h_{ef}:

h_{ef} = nominal stud length − head height − weld burnoff + plate thickness (if plate is flush to the concrete surface)

$= 2.125 - (0.5 + 0.125) + 0.5 = 2.0$

$h_{ef}/d = 2.0 / 0.5 = 4.0$

Therefore, pryout is likely.

$y/d = 16$; ψ_y factor is applicable.

Determine steel capacity:

$V_s = n\,A_s f_{ut}$

$= (4)(0.2 \text{ in.}^2)(65 \text{ ksi})$

$= 52$ kips

$\phi V_s = (0.65)(52) = 33.8$ kips

Determine concrete pryout capacity:

y-spacing factor:

$$\psi_y = \frac{\sqrt{y}}{4d} = \frac{\sqrt{8}}{(4)(0.5)} = 1.41$$

$$V_{po} = 215\lambda\,\psi_y\, n\,\sqrt{f'_c}\,(d)^{1.5}(h_{ef})^{0.5}$$

$$= 215(1.0)(1.41)(4)\sqrt{5000}\,(0.5)^{1.5}(2.0)^{0.5}\left(\frac{1 \text{ kip}}{1000 \text{ lbs}}\right)$$

$= 42.9$ kips

$\phi V_{po} = (0.85)(42.9) = 36.4$ kips

Steel capacity controls and, therefore, V = 33.8 kips.

Problem 2

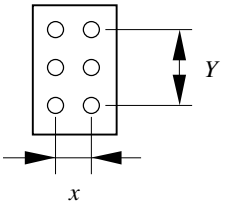

Given:

6 – ½ in. diameter × 2⅛ nominal headed studs
F_{ut} = 65 ksi (per AWS)
x = 4 in., y = 4 in., Y = 8 in.
f'_c = 5000 psi, ½ in. thick plate

Problem:

Find the connection capacity away from all edges.

Solution:

Determine h_{ef}:

h_{ef} = 2.0 (from Problem 1)

$h_{ef}/d = 2.0 / 0.5 = 4.0$

Therefore, pryout is likely.

$y/d = 8$; ψ_y factor is applicable.

Determine steel capacity:

$V_s = n\,A_s f_{ut}$

$= (6)(0.2 \text{ in.}^2)(65 \text{ ksi})$

$= 78$ kips

$\phi V_s = (0.65)(78) = 50.7$ kips

Determine concrete pryout capacity:

y-spacing factor:

$$\psi_y = \frac{\sqrt{y}}{4d} = \frac{\sqrt{4}}{(4)(0.5)} = 1.0$$

$$V_{po} = 215\lambda\,\psi_y\, n\,\sqrt{f'_c}\,(d)^{1.5}(h_{ef})^{0.5}$$

$$= 215(1.0)(1.0)(6)\sqrt{5000}\,(0.5)^{1.5}(2.0)^{0.5}\left(\frac{1 \text{ kip}}{1000 \text{ lbs}}\right)$$

$= 45.6$ kips

$\phi V_{po} = (0.85)(45.6) = 38.8$ kips

Concrete capacity controls and, therefore, V = 38.8 kips.